5-2013

Power Efficient Restart-Capable Acrylonitrile Butadiene Styrene-Based Arc Ignition for Hybrid Rocket Motors

Nathan R. Inkley
Utah State University

POWER EFFICIENT RESTART-CAPABLE ACRYLONITRILE BUTADIENE STYRENE-BASED ARC IGNITION FOR HYBRID ROCKET MOTORS

by

Nathan R. Inkley

A report submitted in partial fulfillment
of the requirements for the degree

of

MASTER OF SCIENCE

in

Aerospace Engineering

Approved:

Dr. Stephen A. Whitmore Major Professor	Dr. David Geller Committee Member

Dr. R. Rees Fullmer
Committee Member

UTAH STATE UNIVERSITY
Logan, Utah

2013

Abstract

Power Efficient Restart-Capable Acrylonitrile Butadiene Styrene-Based Arc Ignition for Hybrid Rocket Motors

by

Nathan R. Inkley, Master of Science

Utah State University, 2013

Major Professor: Dr. Stephen A. Whitmore
Department: Mechanical and Aerospace Engineering

Hybrid rocket ignition has historically involved either dangerous energetic materials or inefficient and failure-prone plasma sources. The vast majority of such systems cannot support multiple restart cycles, thus limiting the applicability of hybrid rockets–especially for in-space propulsion. During research investigating its use as a fuel for hybrid rockets, it was discovered that Acrylonitrile Butadiene Styrene (ABS) plastic possesses unique electrical breakdown characteristics. During a properly designed breakdown event, application of a strong electric field induces a high-temperature arc along the surface of the ABS, concurrent with rapid production of hydrocarbon vapor. This behavior forms the basis of a novel ABS arc ignition system. Several such systems were designed, built and tested. Minimum conditions for successful operation were discovered, including minimum ignition pressure and electrical power requirements. Hands-off restart capability was demonstrated repeatedly. Finally, paths of inquiry for future research are outlined.

(64 pages)

Public Abstract

Power Efficient Restart-Capable Acrylonitrile Butadiene Styrene-Based Arc Ignition for Hybrid Rocket Motors

by

Nathan R. Inkley, Master of Science

Utah State University, 2013

Major Professor: Dr. Stephen A. Whitmore
Department: Mechanical and Aerospace Engineering

Historically, hybrid rocket ignition has been dangerous and unreliable. The vast majority of such igniters are incapable of restarting without exchanging hardware. A restartable igniter without toxic or explosive hazards is desirable. While investigating the potential of ABS plastic to be used as a hybrid rocket fuel, it was discovered that its response to a strong electric field is unique; arcing is observed along with the production of gaseous fuel from the surface of the ABS. The essential ingredients for combustion are heat, fuel, and oxidizer, so it was speculated that this behavior could be used to design a hybrid rocket igniter. Several such igniters were designed, built, and tested. The limitations of such an igniter were outlined, and successful operation was demonstrated many times.

For my mother, Alyssa Inkley

Acknowledgments

None of this research could have taken place without the assistance of my Major Professor, Dr. Stephen Whitmore. I will remember his indefatigable work ethic and intense enthusiasm throughout my career.

It would be remiss of me not to also thank the other members of Dr. Whitmore's research team: Daniel Merkley (and his wife Wendy), Shannon Eilers, Sean Walker and Brittany Chamberlain.

Finally, I thank my wife Theresa. Without her my life would be in a sorry state!

Nathan R. Inkley

Contents

List of Tables

List of Figures

Acronyms

ABS	acrylonitrile butadiene styrene
ESD	electrostatic discharge
APCP	ammonium perchlorate composite propellant
HTPB	hydroxyl-terminated polybutadiene
TEA-TEB	triethylaluminum-triethylborane
PVC	polyvinyl chloride
AM	additive manufacturing
FDM	fused deposition modeling
USU	Utah State University
GOX	gaseous oxygen
HVPS	high voltage power supply
MoNSTeR	mobile nitrous oxide supply and test resource
KRMT	kart for reactive monopropellant testing
P& ID	plumbing and instrumentation diagram
HAN	hydroxylammonium nitrate

Nomenclature

$[\ ]$	Species concentration
$[n_f]$	Fuel partial pressure
α	Thermal diffusivity
$\dot{m}$	Mass flow rate
$\dot{Q}_{Joule}$	Rate of Joule heating
γ	Specific heat ratio
ρ	Density
σ	Electrical conductivity
$\tilde{\alpha}$	Townsend's first ionization coefficient
$\tilde{\gamma}$	Townsend's second ionization coefficient
$\tilde{k}$	Thermal conductivity
A	Area
A^*	Throat area
c_p	Constant-pressure specific heat
d	Electron separation distance
E	Electric field strength
E_a	Activation energy
I	Electrical current
I_0	Pre-breakdown ambient charge saturation current
k	reaction rate constant
k_0	Preexponential factor
M	Mach number
p	Intra-electrod gas pressure
P_0	Stagnation pressure
P_e	Exit pressure
q''	Heat flux

R	Electrical resistance
R	Universal gas constant
r_f	Fuel reaction rate
T	Temperature
T_0	Stagnation temperature
T_p	Reaction product temperature (flame temperature)
T_r	Reactant temperature
T_{ig}	Autoignition temperature
u	Quasi-one-dimensional flow velocity
V	Voltage
V_L	Laminar burning velocity
V_B	Breakdown voltage

Chapter 1

Introduction

In order to appreciate the novelty of the proposed acrylonitrile butadiene styrene (ABS)-based hybrid rocket arc ignition system a theoretical foundation must be laid. First, an outline of the essential features of hybrid propellant rocket motors is provided. Their advantages and disadvantages relative to other forms of rocket propulsion will be outlined. Next, a summary of the state-of-the-art of ignition engineering is given. The high-voltage engineering necessary for the analysis of the arc-igniter is provided. A summary is then made of the design and results of a series of proof-of-concept experiments. Finally, the implications of the experimental results are discussed and recommendations made for further development of the igniter concept.

1.1 Hybrid Rocket Fundamentals

Chemical rocket propulsion systems use a nozzle to convert the heat produced by oxidation-reduction reactions into kinetic energy. Such systems can be broadly categorized by the physical phase in which the fuel and oxidizer are stored. In the vast majority of modern propulsion systems the propellants are all in the same phase; either in solid or liquid form.

Each storage method carries its own advantages and disadvantages. Liquid propellant engines are more efficient and can be throttled, but often require complex turbomachinery and refrigeration. They are typically used for applications in which high efficiency is prioritized above operational flexibility (e.g. orbital launch vehicles). A simplified systems-level diagram for a gas generator cycle liquid bipropellant engine follows in Fig. 1.1.

Solid propellant motors, on the other hand, are relatively simple and can be stored in a launch-ready condition for decades, but lack the ability to throttle or restart. They are

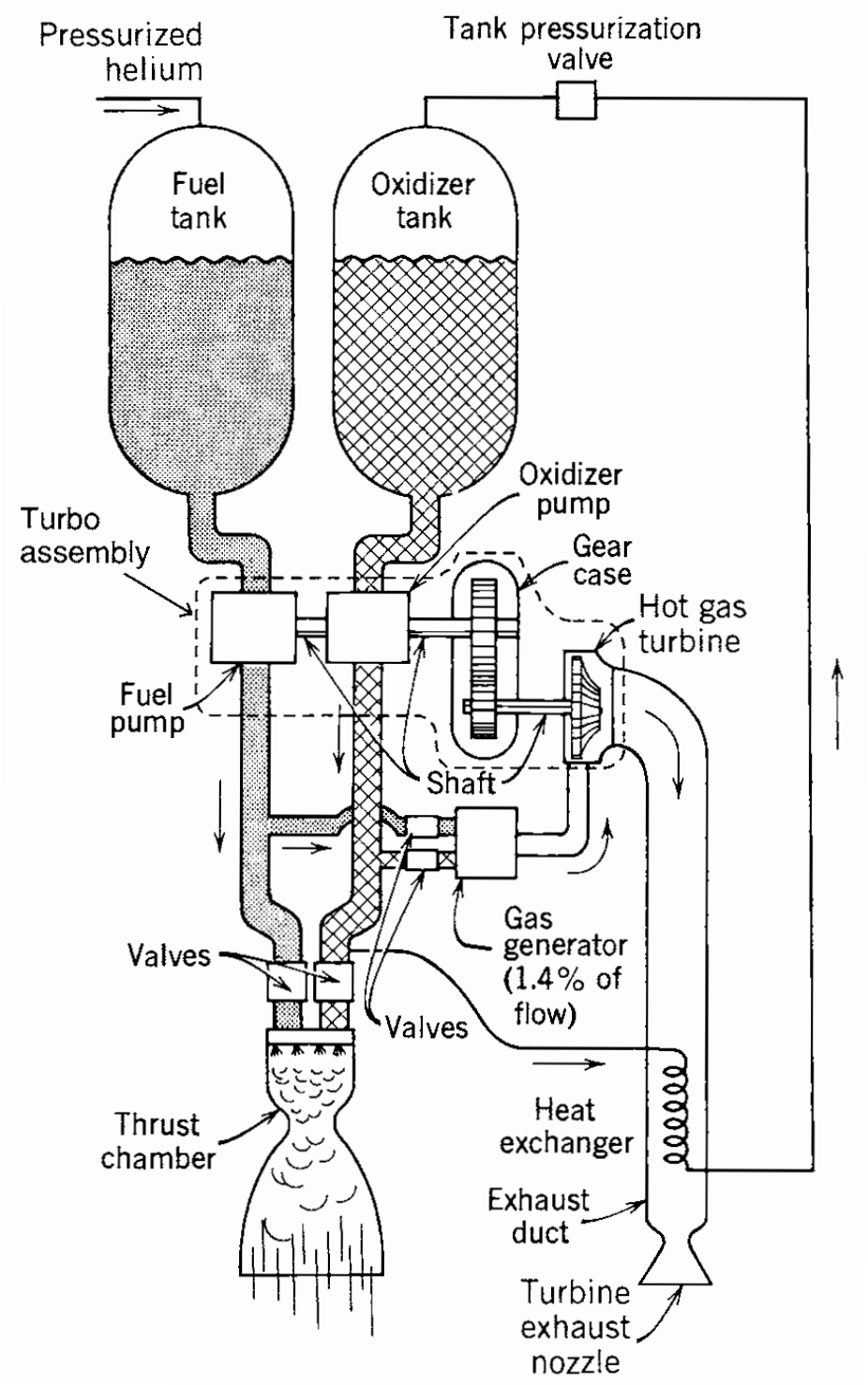

Fig. 1.1: Simplified schematic of a gas generator cycle liquid engine. (Courtesy of Oscar Biblarz)

commonly used in military applications to propel missiles or provide auxiliary thrust for short takeoffs. The typical layout of a solid propellant motor is found in Fig. 1.2

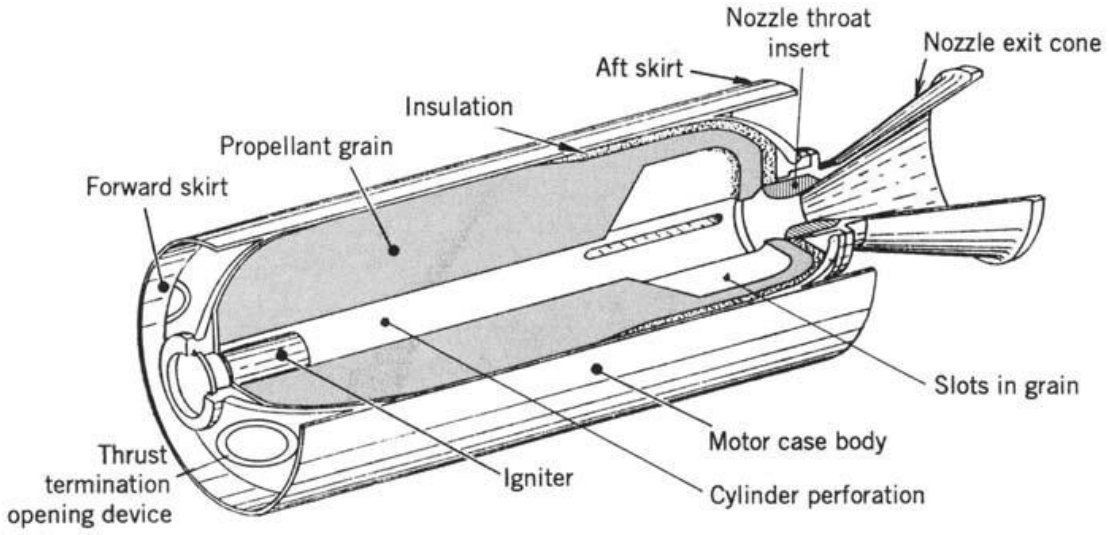

Fig. 1.2: Simplified schematic of a typical solid propellant rocket motor. (Courtesy of Oscar Biblarz)

Hybrid rockets are unique in that the fuel and oxidizer are of differing phases. Most commonly the fuel is cast into a solid grain and the oxidizer is stored as a liquid. In such a motor concept, the oxidizer is usually injected into a precombustion chamber before entering one or more of the fuel grain's axial combustion ports [1]. See Fig. 1.3 for a systems-level diagram of a hybrid rocket motor.

1.2 Advantages and Disadvantages of Hybrid Rockets

Hybrid rockets are unique in that they combine several of the desirable qualities of both solid and liquid propellant systems. However, they also exhibit some unique technological difficulties.

As twenty-first century society becomes more environmentally conscious the use of certain common rocket propellants is being reevaluated [2]. Among liquid propellants, there has been growing concern over highly toxic hypergolics such as hydrazine (N_2H_4) and nitrogen tetroxide (N_2O_4). The loading of such propellants generally requires expensive safety

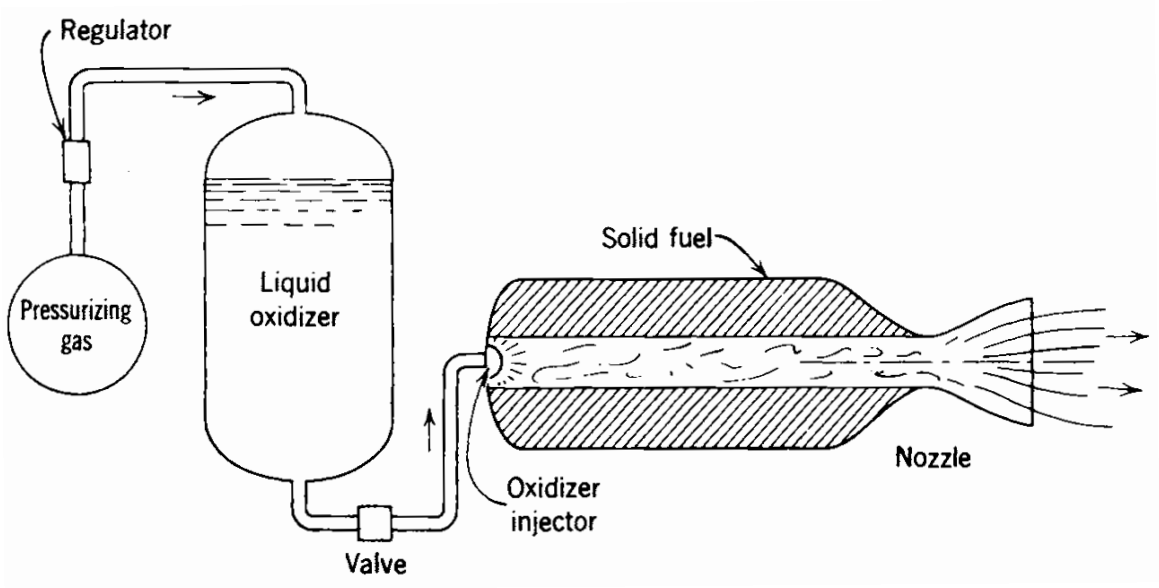

Fig. 1.3: Simplified schematic of a typical solid propellant rocket motor. (Courtesy of Oscar Biblarz)

measures, as exposure to open containers causes chemical burns and can damage several groups of internal organs [3]. Solid propellants have their fair share of environmental issues as well; aside from the obvious hazard of unplanned detonation due to electrostatic discharge (ESD) or sudden compression, the exhaust products of many propellant formulations produce hazardous chemicals. Take, for example, ammonium perchlorate composite propellant (APCP). APCP is used in a wide range of applications: from solid rocket boosters on orbital launch vehicles to small hobby rockets. The exhaust from APCP motors generally contains water, carbon dioxide (CO_2), hydrogen chloride (HCl), and metal oxides. Unfortunately, the hydrogen chloride readily combines with water into corrosive hydrochloric acid.

In contrast, practically all hybrid rocket propellant combinations that have heretofore been put into service posses no detonation hazard, require no special handling, and are relatively benign [4]. Sierra Nevada Corporation's RocketMotorTwo, currently under development for the SpaceShipTwo vehicle, makes use of such a propellant combination: hydroxyl-terminated polybutadiene (HTPB) fuel and nitrous oxide (N_2O) oxidizer.

Unlike solid rocket motors, hybrid rockets are capable of precision throttling. Such capability was demonstrated successfully by Peterson [5], who deep-throttled an 800-lbf

hybrid motor to less than twenty-five percent thrust rating in a closed-loop control system. This ability opens a range of possible applications in which throttling is necessary, but the complications of a liquid propellant system would be undesirable [6].

Unfortunately, hybrid rocket motors carry several critical drawbacks that have negatively impacted their penetration into the aerospace market. Due to the fact that the regression of the propellant grain of hybrid rockets is coupled to oxidizer mass flux rather than combustion chamber pressure (as is the case with solid rockets), the regression rate of hybrids is generally less than one-third that of solid propellant rockets [1]. As a consequence, for hybrid motors to obtain equivalent thrust, the area of the combustion port(s) must be increased. This can be achieved either by lengthening the fuel grain or by increasing the number of combustion ports. Lengthening the fuel grain can fundamentally change the form factor of the system, thus rendering hybrids impractical where compactness is important. Alternatively, increasing the number of combustion ports increases the amount of propellant "slivers" that remain after the fuel has regressed to the motor case, effectively increasing the dry mass of the vehicle.

Finally, the combustion of propellants in hybrid rockets must be initiated by an igniter that provides sufficient heat to cause pyrolysis of the solid fuel grain at the head end of the motor. Consequently, hybrid rocket ignition systems have historically been less robust and reliable than those of most solid and liquid propellant rockets. Ignition of hybrids is typically performed with either pyrotechnic charges or through injection of hypergolic fluids into the combustion chamber [1]. Neither of these methods lends itself to restart-capable operation. The fact that current hybrid motor ignition systems involve no restart capability–or in the best case, a limited number of restarts–has diminished their perceived utility for in-space propulsion.

1.3 Current Applications of Hybrid Rockets

Hybrids are featured prominently in several cutting edge projects. The first privately developed vehicle to carry humans into space, Scaled Composite's SpaceShipOne, was propelled by a hybrid rocket motor [4]. SpaceShipOne was dropped from a high-altitude carrier

aircraft, at which point it ignited its motor and carried out a suborbital mission. SpaceShipOne's successor, SpaceShipTwo, also uses a hybrid motor. Powered flight tests are currently underway.

Hybrid rocket propulsion also plays an important role in Sierra Nevada Corporation's Dream Chaser lifting body vehicle. Dream Chaser will be launched vertically on a ULA Atlas V, perform on-orbit operations such as ferrying crew to and from the International Space Station, and then land horizontally on a runway. Its primary in-space propulsion is provided by two hybrid rocket motors with HTPB fuel and nitrous oxide oxidizer [7].

In both of the aforementioned modern applications, the ability to carry out an infinite number of restart cycles would be beneficial. With a finite number of restarts, Dream Chaser will not be able to react as flexibly to unexpected situations on orbit. SpaceShipTwo could also benefit from the ability to restart its motor in the event of a botched landing attempt. Infinite restart capability carries dramatic implications for operational flexibility and mission safety.

Chapter 2

Rocket Ignition Fundamentals

2.1 Chemical Kinetics

Propulsion engineering commonly makes use of thermodynamics to predict the composition and properties of a reactive mixture. While thermodynamic analysis provides valuable information about steady-state operation, it gives no information about the rate at which reactions may proceed or how rapidly the steady-state is approached. Ignition is a transient process by definition, so chemical kinetics is necessary to perform useful analyses.

Let us consider a general chemical reaction. Let the reactants be denoted as A and B, while the products are C and D. The stoichiometric coefficients necessary to balance the chemical equation are a, b, c, and d; each corresponding to its uppercase counterpart. The reaction can be written as:

$$aA + bB \rightarrow cC + dD \tag{2.1}$$

According to the rate law of chemical kinetics, the rates of destruction of the reactants and the rates of formation of the products are given by the following equations:

$$\frac{d[B]}{dt} = -bk[A]^a[B]^b \tag{2.2}$$

$$\frac{d[A]}{dt} = -ak[A]^a[B]^b \tag{2.3}$$

$$\frac{d[C]}{dt} = ck[A]^a[B]^b \tag{2.4}$$

$$\frac{d[D]}{dt} = dk[A]^a[B]^b \tag{2.5}$$

where k is the reaction rate constant, and brackets signify concentration.

For reversible reactions, the "backwards" reaction rate can be similarly found. This is useful for solving problems of thermodynamic equilibrium.

The rate constant, k, is found via the Arrhenius Equation:

$$k = k_0 e^{-E_a/(RT)} \tag{2.6}$$

where k_0 is the so-called preexponential factor and E_a is the reaction's activation energy. These two constants are determined experimentally for reactions of interest. R is the universal gas constant and T is the absolute temperature.

Several relevant observations can be made at this point. For a reaction with a given preexponential constant and activation energy, the rate at which the reaction occurs is a function of only pressure (i.e. concentration) and temperature. According to collision theory, macroscopic chemical reactions are the result of the collision and recombination of microscopic reactant particles. At higher pressures the concentration of reactants is greater, and thus the likelihood of collisions increases. The rate of reaction then correspondingly increases. Alternatively, as temperature is increased, a greater proportion of reactant particles will posses the energy necessary for a collision to result in a recombination event, also augmenting reaction rate [8].

2.2 Ignition

For successful ignition to take place, the amount of heat generated by combustion must exceed the amount of heat lost to the flame's surroundings. Techniques have been developed which, given certain simplifying assumptions, enable quantification of flame propagation [8].

For the purposes of gaining a qualitative understanding of combustion, let us examine a simplified flame propagation model. The process of interest is a one-dimensional, steady, reacting compressible flow problem. The equations of state are the compressible conservation laws for reacting flows. We assume laminar flow conditions and premixed reactants. While the vast majority of ignition scenarios involve turbulent flow and realistic diffusive flames, the laminar premixed case still illustrates the basic trends at play. We also make

several simplifying assumptions about the gradient nature of heat flux due to mass diffusion and chemical reaction rate. This solution was first obtained by combustion physics pioneers Ernest-Francois Mallard and Henry Louis Le Chatelier and later refined by modern researchers [8]. The laminar burning velocity is given by:

$$V_L = \sqrt{\frac{(\alpha r_f/[n_f])(T_p - T_{ig})}{T_{ig} - T_r}} \tag{2.7}$$

with

$$\alpha = \frac{\tilde{k}}{\rho c_p} \tag{2.8}$$

where α is the thermal diffusivity, $\tilde{k}$ is the thermal conductivity, c_p is the constant-pressure specific heat, r_f is the reaction rate of the fuel as given by the kinetics rate equation, $[n_f]$ is the partial pressure of the fuel, T_p is the temperature of the reaction products, T_{ig} is the ignition temperature of the reactant mixture, and T_r is the initial temperature of the reactant mixture. The rate of energy release generated by combustion can now be calculated simply as:

$$q'' = \rho V_L c_p \Delta T_f \tag{2.9}$$

where ΔT_f is the temperature rise across the flame. We see that the heat flux due to combustion is a function of thermal diffusivity, reaction kinetics, flame temperature, ignition temperature, and initial reactant temperature.

If heat and mass transfer away from the flame are great enough, the temperature and reactant concentrations will be lowered, which in turn slows the reaction rate. As the reaction rate is retarded, heat generation from combustion decreases, and the flame may be quenched. Thus we see that insufficient reaction rates or excessive heat and mass transfer during ignition may result in failure to initiate primary combustion.

2.3 Commonplace Spark Ignition Systems

Restart-capable spark ignition systems are a common feature of modern life. Most people encounter them on a daily basis in the form of car, aircraft, or small gasoline engines.

Commonly they take the form of premixed turbulent-flow systems.

In such systems, a practically homogeneous mixture of fuel and air is created and injected into the combustion chamber either through venturi carburation or fuel injection. In a four-stroke engine, the premixed reactants enter the cylinder during the intake stroke, and are then compressed as the piston moves toward top dead center. At this point, high-voltage gas breakdown is initiated at the spark plug. Combustion reaction rates in the cylinder are engineered to be high due to the arc's high temperature and the high reactant concentration created during the compression stroke.

Gas turbine cycles are thermodynamically similar to gas piston engines, and make use of a similar spark plug ignition system. The primary difference between the two lies in the method by which the pressure of the reactant mixture is increased, which in a turbine cycle is performed by a series of spinning compressor blades.

2.4 Rocket Ignition

Rocket engines and motors make use of a fundamentally different technique to create high pressures in the combustion chamber. No moving mechanical contrivances are involved; high pressure is maintained due to the choking mass flow conditions that arise from compressible fluid dynamics.

Consider the convergent-divergent nozzle in Fig. 2.1. Upstream of the throat there exists gas with a certain stagnation pressure, P_0. Downstream of the nozzle exit is an ambient pressure, P_e. As the ratio of these two pressures (P_0/P_e) is increased from unity, flow will accelerate in the converging section up to a maximum subsonic velocity at the throat before decelerating in the diverging section. Up to a point, the mass flow rate will increase as the pressure ratio is increased. Once sonic flow is achieved at the throat, however, the flow's quasi-one-dimensional characteristics change. As the pressure ratio is increased even further, the flow at the throat remains sonic, while the downstream flow is accelerated rather than decelerated in the diverging section. This behavior is dictated by the area-velocity relation for compressible flow, which is derived from the differential form

of the conservation laws:

$$\frac{dA}{A} = (M^2 - 1)\frac{du}{u} \tag{2.10}$$

where A is cross-sectional area, M is Mach Number, and u is the flow velocity [9]. At this point the flow conditions upstream of the throat are decoupled from those of the the supersonic downstream flow section. There is now a certain fixed mass flow rate for a given stagnation pressure and temperature that is in no way impacted by the external pressure:

$$\dot{m} = \frac{P_0 A^*}{\sqrt{T_0}} \sqrt{\frac{\gamma}{R} \left(\frac{2}{\gamma + 1} \right)^{(\gamma+1)/(\gamma-1)}} \tag{2.11}$$

where A^* is the throat area, γ is the specific heat ratio for the gas, and R is the gas constant [9].

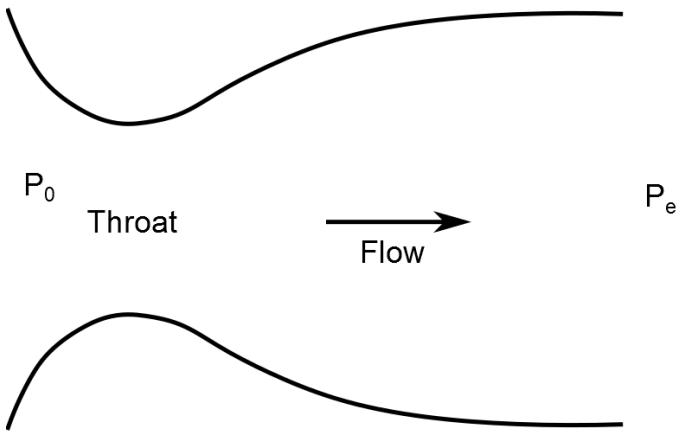

Fig. 2.1: Schematic of a convergent-divergent nozzle.

This behavior carries important consequences for ignition. Should uncombusted propellants be allowed to "choke" the thrust chamber prior to ignition, an excessive spike in chamber pressure will commence once combustion begins. This is known colloquially as a "hard start" and often leads to a rapid unplanned disassembly of the rocket. Avoidance of "hard starts" requires careful experimentation and run sequence timing to reliably control the production of hot gas [1].

A variety of rocket ignition systems have been implemented. Monopropellants make use of a catalyst bed to dramatically lower required activation energy and initiate decomposition. Hypergolic propellants spontaneously ignite as soon as the oxidizer and fuel come into contact. For non-hypergolic bipropellant systems pyrotechnic or pyrophoric charges are the norm. A survey of common rocket ignition techniques follows.

2.4.1 Monopropellants

Monopropellants consist of a mixture of an oxidizing agent and combustible matter. In operation, the monopropellant is run through a catalyst bed which initiates exothermic decomposition. The reaction products are then expanded through a nozzle to produce thrust. Monopropellant thrusters are commonly used for orbital maneuvering because of their compactness, storability, and ease of operation [1]. Unfortunately, they are generally extremely toxic substances. Common examples include hydrazine (N_2H_4) and nitrogen hydrogen peroxide (H_2O_2).

2.4.2 Hypergolic Propellants

Hypergolic propellants consist of a fuel and oxizdizer that are self-igniting, that is, combustion is initiated as soon as the fuel and oxidizer come into contact. They require no ignition system and are extremely reliable. Unfortunately, hypergolics are extremely toxic and the use of such propellants on a large scale carries negative environmental consequences. Common hypergolic propellants include hydrazine and nitrogen tetroxide (N_2O_4) [10].

2.4.3 Pyrotechnic Ignition

Solid explosives or small pellets of high-burn exponent propellant to produce heat and gas necessary to ignite a solid rocket motor. The energetic material can be contained in a variety of configurations: bag, basket, plastic case, perforated tube, roll, string, or sheet. They can also be used as initiator stages for larger pyrogen igniters. The layout of a basket pyrotechnic igniter is shown in Fig. 2.2 below. Common energetic materials for pyrotechnic igniters include boron potassium nitrate ($BKNO_3$) [11].

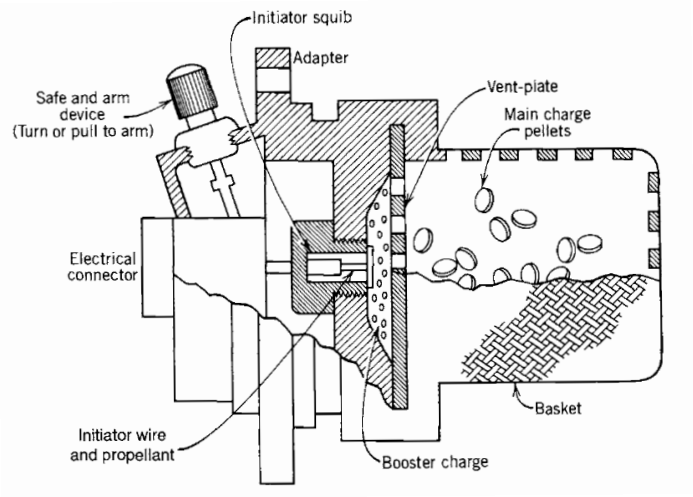

Fig. 2.2: Schematic of a typical pyrotechnic igniter.

2.4.4 Pyrogen Igniters

Essentially, a pyrogen igniter is a small solid-propellant rocket motor that is designed to produce hot gases that impinge on the surface of a primary solid propellant grain. The igniter itself is typically initiated with electrical heating, and may consist of multiple stages, each growing in size and energy output [12]. Most large solid rocket motors and many liquid propellant engines make use of such ignition systems [1]. Obviously, pyrogen igniters can only be used once. Fig. 2.3 shows the first stage motor of the Pegasus air-launched satellite launch vehicle, which employs a common head-end pyrogen igniter integration scheme.

2.4.5 Auxiliary Fluid Ignition

During ignition, hypergolic fluids can be injected into the combustion chamber along with the primary propellants. The energy and hot gas generated by the short reaction of the hypergolics provides the initial conditions necessary for self-sustaining combustion of the primary propellants to take place. Triethylaluminum-triethylborane (TEA-TEB) mixtures are a very common auxiliary ignition fluid [13]. Auxiliary fluid injection systems have the potential to support multiple restarts, as in Space Exploration Technology's Merlin 1-D engine [14]. Fig. 2.4 contrasts the color of the TEA-TEB ignition plume and the post-ignition kerosene/liquid oxygen flame. The TEA-TEB reaction's unique green color is

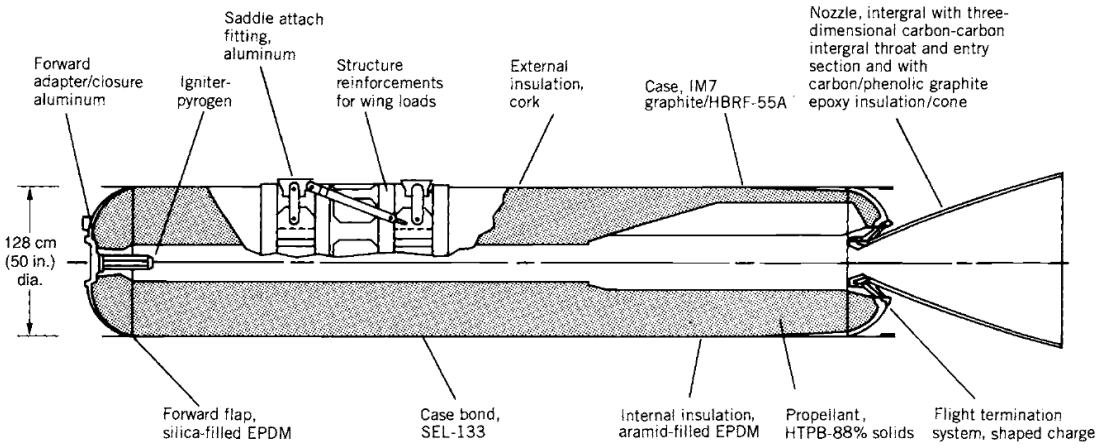

Fig. 2.3: Schematic of the first stage motor of Orbital Sciences' Pegasus launch vehicle, featuring a pyrogen igniter (Credit: Orbital Sciences and ATK Launch Systems via Oscar Biblarz).

characteristic of boron compounds.

2.4.6 Plasma Torch Ignition

Plasma torches are devices for generating a directed flow of plasma, and have been effectively used for gas turbine engines and supersonic combustion ramjets for ground test articles [15]. They produce very high output temperatures, but have a low total mass flow. Achieving a high total enthalpy output requires a large input power. Typically, the power production units (PPU) for these devices are bulky, and not appropriate to flight applications. Originally, Space Exploration Technologies designed the Merlin Engine to ignite using a plasma torch, but later abandoned the concept in favor of pyrophoric ignition to lower the input energy requirements and simplify the overall systems design [16].

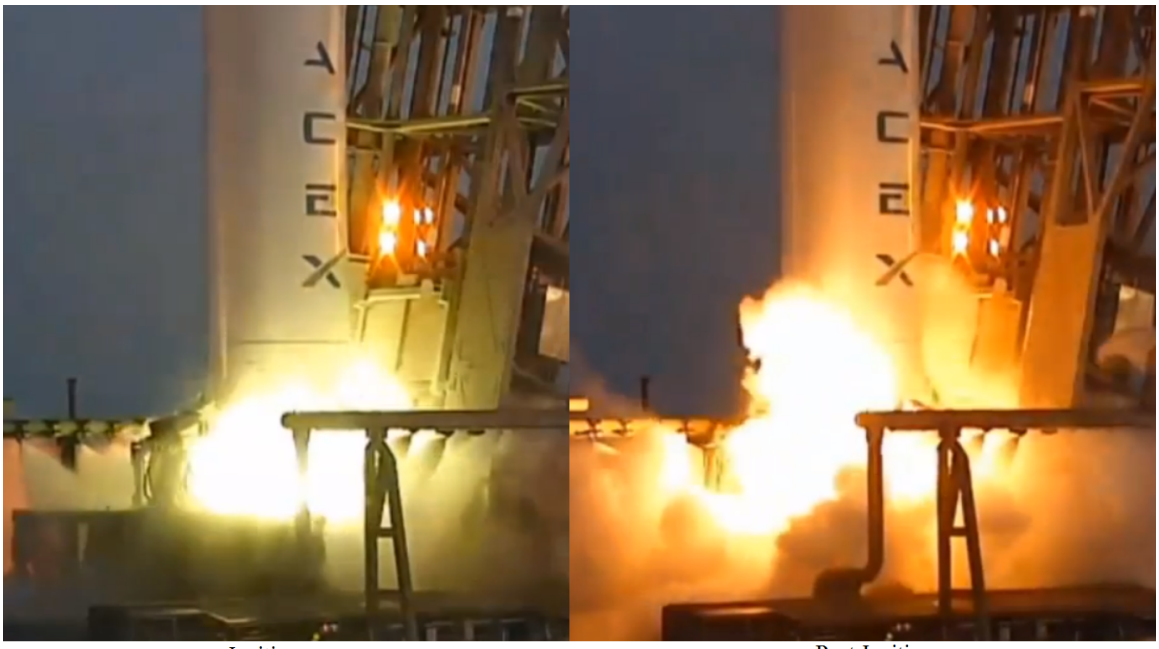

Fig. 2.4: Comparison of Merlin 1D flame color during and after TEA-TEB injection.

Chapter 3

High-Voltage Breakdown

If sufficiently high voltage is applied across an insulator, a swift increase in conductivity will result. This event is referred to as electrical breakdown. The voltage at which an insulator suffers electrical breakdown is called the breakdown voltage. Though the nature of the physical mechanisms vary, electric breakdown has been observed in solids, liquids, and gases [17].

The ability to predict and model electrical breakdown has multiple engineering applications. For example, finding an appropriate spark gap or electrode material when designing spark ignition systems. For other applications, being able to quantify the risk of electric breakdown may be desirable. The remainder of this chapter will review the physical mechanics of electrical breakdown in gases and, to a lesser extent, solids.

3.1 Electrical Breakdown in Gases

Gaseous electrical breakdown is frequently encountered in everyday life. It often produces an electric arc; a continuous path of hot plasma that connects two electrodes. Lightning is a spectacular natural example of electrical breakdown in a gas. The spark between a doorknob and a persons fingertip is a more mundane example.

3.1.1 Pre-Breakdown Ionization and Decay

Generally speaking, gases are very effective insulators. There does exist, however, a certain non-zero steady-state density of charged particles in otherwise neutral gases–in fact, air at STP does posses a measurable conductivity [17]. This is caused by ionization of molecules due to cosmic or terrestrial radiation sources. Without an electric field imparting energy to the charged particles the rate of ion generation from radiation sources is

counteracted by natural decay processes, leading to a steady state charge density.

Consider two parallel plate electrodes surrounded by a gas. Beginning with no potential difference, the voltage between the electrodes is gradually increased, while current is simultaneously measured. As depicted in Fig. 3.1, the current initially increases, but quickly reaches a saturation level that is related to the charge density of the gas. As the voltage is increased beyond a certain value, however, the current between the electrodes grows exponentially towards infinity–practically a short circuit. This behavior was first observed experimentally by Paschen in the late nineteenth century [18].

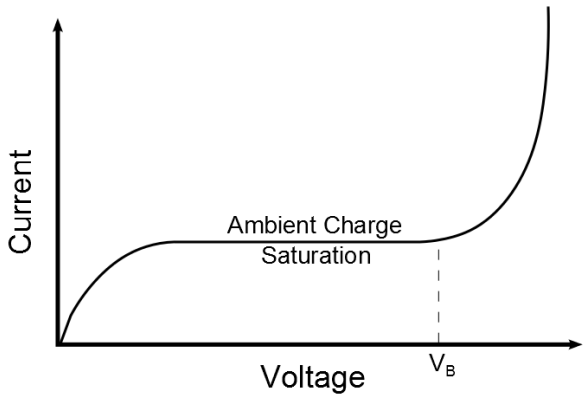

Fig. 3.1: Conceptual pre-breakdown current-voltage relationship in ordinary gas.

Given a sufficiently strong electric field, ambient charged particles in a gas can be accelerated such that some collisions between charged particles and neutral molecules will result in ionization of the neutral molecule. In high voltage engineering parlance this is known as primary emission. The newly liberated electrons will now be accelerated by the electric field and produce progeny of their own. This phenomenon is referred to as a Townsend Avalanche [17].

The positive ions created during primary emission processes will be accelerated toward the cathode, whose bombardment results in the production of more free electrons. Additionally, electrons are generated at the cathode via the photoelectric effect and thermionic

emission. This is called secondary emission. It is worth noting that secondary emission is highly dependent on the cathode material; some materials are more prone to giving up electrons than others [17].

In order to quantify the current, two constants relating to ion production must be defined. First, $\tilde{\alpha}$ is the number of new electrons generated by an electron per unit distance in the direction of the electric field. Second, $\tilde{\gamma}$ is the number of electrons produced at the cathode per impact by a positive ion. Together these quantities are known as the Townsend ionization coefficients.

Electron creation from both primary and secondary processes can be combined to obtain an expression for the pre-breakdown current between the electrodes [17]:

$$I = \frac{I_0 e^{\tilde{\alpha} d}}{[1 - \tilde{\gamma}\,(e^{\tilde{\alpha} d} - 1)]} \tag{3.1}$$

where I is the current and d is the distance between the anode and cathode. The essential condition for breakdown can now be found by setting the denominator to zero, producing infinite current. This means that for breakdown to occur the following statement must be true:

$$\tilde{\gamma}\left(e^{\tilde{\alpha} d} - 1\right) = 1 \rightarrow \tilde{\alpha} d = \ln\left(\frac{1}{\tilde{\gamma}} + 1\right) \tag{3.2}$$

3.1.2 Paschen's Law

From gas breakdown experiments a standard empirical expression for the first Townsend ionization coefficient has been formulated in terms of electric field intensity and gas pressure:

$$\tilde{\alpha} = pAe^{-Bp/E} \tag{3.3}$$

where p is pressure, A and B are experimentally determined constants for a given gas species, and E is the electric field strength. If we assume a uniform field (as is the case for

infinite-area parallel plate electrodes) the electric field strength is simply:

$$E = \frac{V}{d} \tag{3.4}$$

in which V is the potential difference between the electrodes. We now substitute the breakdown condition from Equation 3.2 into the experimental expression for $\tilde{\alpha}$ and solve for V. This yields Paschen's Law:

$$V_B = \frac{Bpd}{\ln(Apd) - \ln[\ln(\tilde{\gamma}^{-1} + 1)]} \tag{3.5}$$

Paschen's law implies that, for a given gas and electrode material, breakdown voltage in a uniform electric field is a function of the product of pressure and electrode separation. Paschen curves for several gases with highly conductive electrodes are plotted in Fig. 3.2. It

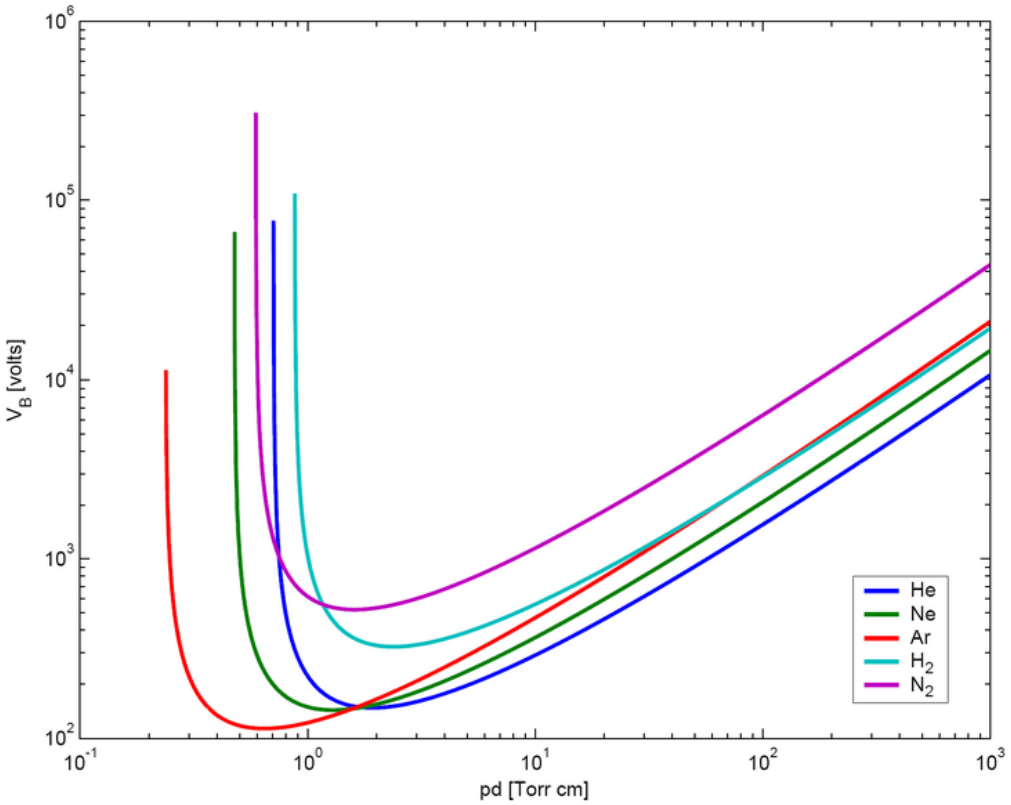

Fig. 3.2: Paschen curves for selected gases.

is worthwhile to note that a minimum breakdown voltage exists. Large values of pd imply a higher probability of collisions between accelerating electrons and neutral molecules. At the same time, however, increasing pd shortens the mean free path of the electrons, effectively limiting the amount of kinetic energy they can accumulate between collisions and decreasing the probability that a collision will result in ionization [19]. Breakdown voltage minima for several gases are given in Table 3.1.2.

3.2 Electrical Breakdown in Solids

The theory of electrical breakdown in solids is not nearly as mature as it is for gases. The mechanisms behind solid breakdown are complex and vary between material type and duration of voltage application [19].

Thermal breakdown is an extremely simple solid breakdown mechanism of particular relevance to the subject of this report. All dielectrics allow the passage of some amount of current, albeit a minute amount. The passage of current through a resistive medium generates heat, which is then transferred throughout the dielectric and eventually to the environment surrounding the dielectric. This is known as "Joule," or simply "resistive" heating. A simple expression for this heat generation in terms of electric field strength and

Table 3.1: Minimum breakdown voltages for selected gases.

Gas	$(V_B)_{min}$ (V)	$(pd)_{min}$ $(torr \cdot cm)$
Air	327	0.567
Ar	137	0.9
H_2	273	1.15
He	156	4.0
CO_2	420	0.51
N_2	251	0.67
N_2O	418	0.5
O_2	450	0.7
SO_2	457	0.33
H_2S	414	0.6

material conductivity is given by:

$$\dot{Q}_{Joule} = E^2\sigma(T) \tag{3.6}$$

where σ is the conductivity as a function of temperature. This equation's similarity to the more common $P = V^2/R$ should be obvious. For most materials, conductivity increases with temperature [17]. If the rate of heat transfer away from the conductive path is is not sufficient to maintain an equilibrium temperature, a condition of thermal (and conductive) instability will follow.

Chapter 4

ABS Igniter Concept

The theoretical underpinnings of the novel igniter concept have now been reviewed. Building upon this foundation, a description of the restartable ABS arc igniter follows in the subsequent sections of this chapter.

4.1 ABS Plastic

4.1.1 ABS Properties

Acrylonitrile butadiene styrene $[(C_4H_8)_x \cdot (C_4H_6)_y \cdot (C_3H_3N)_z]$ is a mass-produced thermoplastic that is growing in relevance as a practical engineering material in for a variety of applications. Raw ABS is cheaply manufactured from propylene and ammonia. It is easily machinable and can be injection-molded. Current applications include plumbing, electrical enclosures, and toys. Some physical properties of ABS are given in Table 4.1.1 [20].

Unlike materials used in similar applications such as acrylic and polyvinyl chloride (PVC), the thermoplastic nature of ABS makes it an ideal material for additive manufacturing (AM). Typically, ABS stock is used for a type of additive manufacturing known as fused deposition modeling (FDM). FDM allows the rapid, precise, and accurate manufacture of complex geometries from several polymeric materials. Similar to many AM techniques,

Table 4.1: Approximate mechanical properties of ABS plastic.

Mechanical Property	Extruded	FDM-Printed
Tensile Strength	41.6 MPa	22 MPa
Tensile Modulus	$2,144$ MPa	$1,627 MPa$
Tensile Elongation	5%	6%
Flexural Strength	$52 - 82$ MPa	41 MPa
Flexural Modulus	$1,538 - 2882$ MPa	$1,834$ MPa

FDM printers are given a part's three-dimensional model, which is then physical produced by printing layer upon layer of thermoplastic.

4.1.2 ABS as a Hybrid Rocket Fuel

ABS possesses economic, physical and thermodynamic properties that make it attractive as a fuel for hybrid rocket motors. Firstly, the material is already in mass-production and therefore is relatively inexpensive (more than 1.4 billion kg of ABS was manufactured in 2010 alone [21]). It has a practically indefinite shelf life. Furthermore, manufacture of fuel grains via FDM precludes the necessity of maintaining expensive fabrication processes involving custom tooling and facilities.

The ability to additively manufacture an ABS fuel grain enables the fabrication of fuel grain geometries that would be impossible to cast or to machine from stock material. As discussed earlier, hybrid rocket motors suffer from a low regression rate as compared to solid propellant rockets. Research carried out by Eilers indicates that novel helical flow path geometries can dramatically increase regression rate and reduce form factor [22]. Manufacture of such a geometries is not feasible using traditional fuel grain production methods. Additionally, due to its high heat capacity and tensile strength, "caseless" hybrid motors have been envisaged which do not require a liner, insulator layer, or motor case. Such designs would reduce part count and aid ease of fabrication.

In terms of performance, it has been shown by Whitmore, et al. that ABS fuel is thermodynamically equivalent to the most prevalent hybrid fuel, HTPB [23]. The research compared ABS and HTPB motors with nitrous oxide oxidizer. Whitmore showed that, although the flame temperature of ABS is somewhat cooler than that of HTPB, its exhaust products have a lower molecular weight. In terms of the ubiquitous propulsion engineering figures of merit, specific impulse (I_{sp}) and characteristic velocity (c^*), there is practically no difference between ABS and HTPB. Furthermore, the regression rates of both fuels were shown to be very similar [23].

4.1.3 Discovery of Unique Electromechanical Characteristics

While the utility of ABS as a hybrid propellant was being researched at Utah State University (USU), it was serendipitously discovered that ABS could be used as an effective electrode in electrical gas breakdowns. Observed in association with the electrical breakdown was the generation of quantities of hydrocarbon vapor from the ABS. Shortly after this discovery, unsuccessful attempts to reproduce it were made with other hybrid fuel materials such as HTPB and paraffin. Fig. 4.1 shows the arc produces in one of the crude early tests. During such early tests it was found that reliable arcing could be achieved with

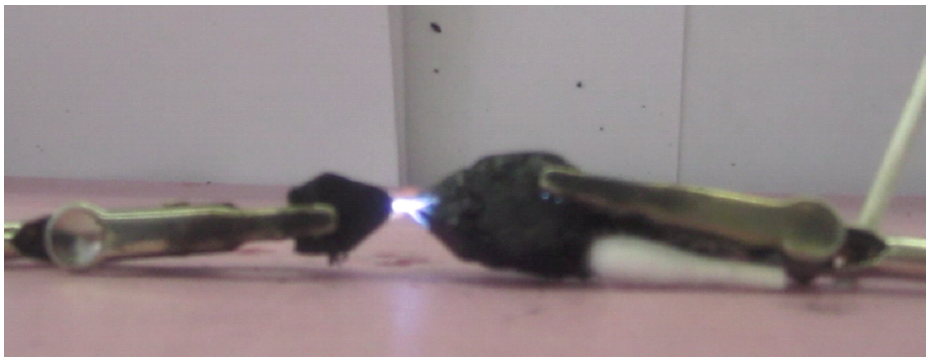

Fig. 4.1: Early electrical gas breakdown experiment with ABS electrodes.

as little as 8 W power input at a voltage of roughly $1,000$ V. In comparison, automobile spark plug ignition coils normally produce $12,000 - 25,000$ V.

4.2 Overview of ABS Arc Igniter Concept

The discovery of ABS' unique breakdown characteristics prompted the invention of an ignition system which takes advantage of the phenomenon. In such an igniter, two conducting paths are embedded within an ABS fuel grain. The conducting paths terminate in electrodes that are flush with the combustion port surface and are therefore exposed to the interior of the combustion chamber. A voltage is applied across the two electrodes. For a properly designed system geometry, the breakdown voltage between the metal electrodes is too high to initiate direct metal-to-metal arcing, rather, arcing will take place between electrodes and the surface of the ABS fuel. Generation of fuel vapor then commences due to

temperature-induced pyrolysis as well as electromechanical and thermal breakdown of the ABS. After some predetermined amount of time has passed, oxidizer is allowed to flow into the combustion chamber. There now exists in the combustion chamber a mixture of gaseous reactants and a source of activation energy (provided by the arc). If the conditions meet the criteria for successful ignition as discussed in Chapter 2, self-sustaining combustion of the reactant mixture will take place. The energy release of the initial combustion reaction then causes pyrolysis along the main fuel grain and finally leads to steady-state combustion along the entire port surface. A rudimentary cross-sectional diagram of a potential ABS arc igniter is shown in Fig. 4.2. A photograph of the phenomenon is found in Fig. 4.3. Fig. 4.4 demonstrates the generation of vaporized hydrocarbons.

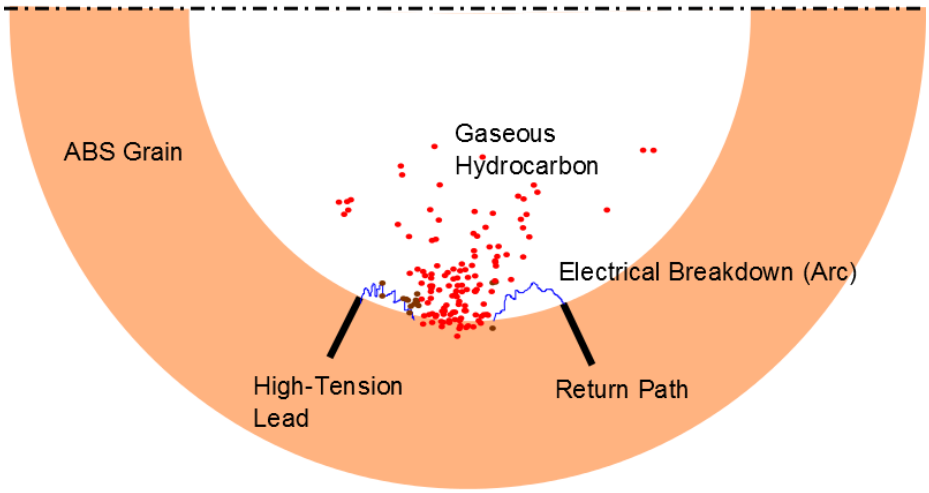

Fig. 4.2: Conceptual cross-sectional diagram of an ABS arc igniter.

4.3 Comparison with Traditional Igniters

A successfully implemented ABS arc ignition system would fundamentally differ from current methods in several regards. First, unlike pyrotechnic, pyrogenic, and pyrophoric ignition systems, the ABS arc igniter involves absolutely no detonation or toxicity hazard.

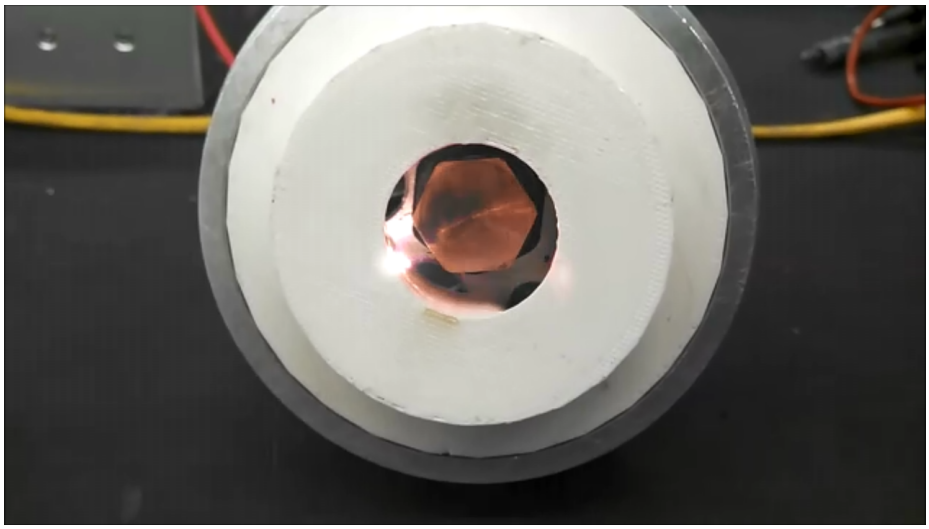

Fig. 4.3: Electrical breakdown in an ABS arc igniter.

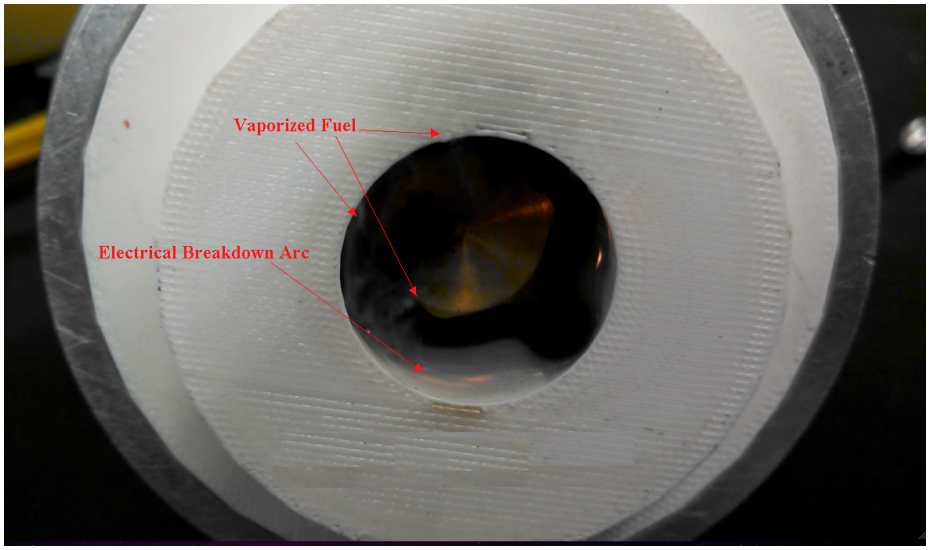

Fig. 4.4: Hydrocarbon vapor production in an ABS arc igniter.

The individual components are commonplace and completely inert, which cannot be said for industry-standard rocket ignition chemicals such as $BKNO_3$ or TEA-TEB. The only significant safety hazard to address in ABS arc igniter operations is the possibility of unintended high voltage discharge. If implemented on a hybrid rocket (the components of which are not generally a detonation hazard) the only risk incurred is that of causing short-circuit of electrical systems or shocking operational personnel. Considering that common inductive coil and capacitive discharge spark ignition systems routinely deal with much higher velocities, such risks are very manageable.

An important difference between the ABS spark igniter and everyday spark ignition systems lies in the function of the electrical gas breakdown. In a commonplace spark ignition system, the arc merely supplies the necessary temperature and activation energy for the compressed fuel-oxidizer mixture to undergo self-sustaining combustion. This is also the case for the ABS arc igniter, however, the arc plays an additional role. In the ABS igniter the arc not only serves to initiate combustion, but also provides increased temperatures for pyrolysis and thermal breakdown of the solid fuel. Thus, in the ABS arc igniter, the arc both generates the fuel vapor for the fuel-oxidizer mixture and provides the activation energy necessary to begin its combustion.

The ability to perform multiple start-stop-restart cycles is desirable in rocket ignition systems. Historically, such capability has been difficult to achieve with non-hypergolic bipropellants. Potentially, ABS arc igniters can be designed in such a way that, as the ABS fuel grain regresses, the electrical breakdown characteristics between the electrodes are maintained. Assuming this is possible, a hybrid rocket motor equipped with such an ignition system would be capable of a practically infinite number of restarts–as long as the ABS grain has not regressed past the entry channels of the conducting paths, the motor should be capable of restarting.

Chapter 5

Experimental Work

5.1 Initial Prototype

Initial efforts to develop a practical ABS arc igniter were spearheaded by Mike Judson, a former graduate research assistant as USU. Fig. 5.1 provides an exploded view of the prototype igniter with the gaseous oxygen (GOX) oxizider flow path proceeding from left to right. The igniter was designed for a target chamber pressure of 125 *psia* with an oxidizer mass flow rate of approximately 5 g/s. In this design, the ABS fuel grain was encased by a cylindrical polycarbonate shell. Two sets of wire (one for the high-tension lead and another for the return path) were embedded within the ABS with one end contacting an aluminum plate and the other end forming an exposed electrode on the fuel grain surface. The ABS fuel element itself was additively manufactured using a Stratasys Dimension® 3-D Fused Deposition Model (FDM) printer. Initially, the high voltage was supplied by a crude off-the-shelf "stun gun." This was soon replaced by an UltraVolt ® 10C high voltage cap-charging power supply. The high voltage power supply (HVPS) is still used to provide the potential difference in ongoing arc ignition efforts, and can deliver a maximum of 15 mA at $10,000\ V$.

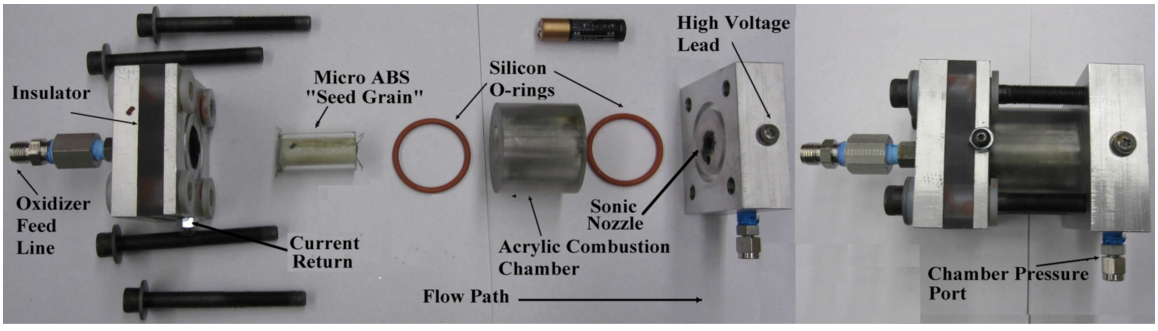

Fig. 5.1: Exploded view of an early ABS arc igniter prototype.

Ignition was reliably achieved for this setup with a mere 8 W at roughly $1,000$ V. During testing of the prototype, it was observed that the voltage necessary to achieve breakdown progressively decreased over many restart cycles. It is theorized that this is due to the accumulation of conducting char material in the interior of the igniter. In total the prototype carried out twenty-seven restart cycles. A still image from one of the prototype's ignition tests is found in Fig. 5.2.

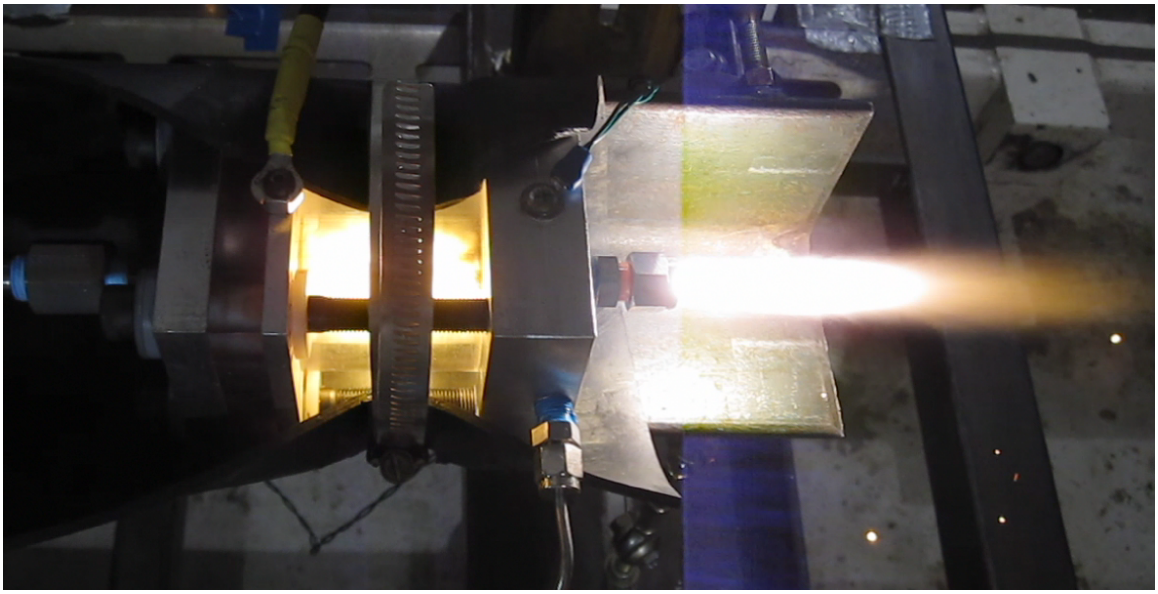

Fig. 5.2: Test of an early ABS arc igniter prototype.

5.2 Large Motor Ignition Demonstrator

The next logical step in the advancement of ABS arc igniter technology was the ignition of a relatively large hybrid motor. The chosen infrastructure for this effort was based on the commercially available Cesaroni® 98-mm solid rocket motor case and motor cap. The large motors for this burn campaign made use of nitrous oxide as oxidizer and either HTPB or ABS as fuel grain material. The motor yielded approximately 800 N of thrust with either type of fuel grain.

Miniaturization of the entire ABS arc igniter system for integration into the head end of the 98-mm motor proved to be a significant engineering challenge. Fig. 5.3 shows a

schematic of the integration of the so-called micro-hybrid igniter. A small ABS fuel element was inserted into a preexisting pyrogenic igniter port. A ceramic insulator was used to isolate the high tension conductive path. A simple injector was machined into the ceramic as well as channels for passing the high tension lead to the ABS fuel grain. Inside of the ABS was a channel with an embedded wire which made contact with the inner surface of the motor cap's igniter port, thus taking the arc's return path through the metal of the motor cap. The plume of the micro-hybrid igniter exited through a sonic graphite nozzle into the main motor's precombustion chamber. Fig. 5.4 shows a test of the mircro-hybrid/motor cap assembly without the main motor.

Six successful static fire tests were carried out with the micro-hybrid igniter apparatus; four with an HTPB main fuel grain, and two with ABS. It is particularly notable that the four tests on the HTPB motor were carried out in rapid succession with absolutely no hardware changes–a rare feat for such a large hybrid rocket motor. The previously observed gradual reduction in breakdown voltage was also present for the micro-hybrid igniter. In the case of the HTPB restart cycles, the breakdown voltage fell from approximately $1,500\ V$ for the first burn to $700\ V$ for the fourth consecutive duty cycle. The average required energy to ignite was $12\ J$ with a power draw of $9\ W$.

Unfortunately, the the micro-hybrid igniter design suffered from several critical flaws. Due to the form factor restraints of the motor cap, the maximum allowable diameter of the ABS igniter fuel grain was only $1.25\ cm$. Regression of the igniter grain during operation, though slow, represented a large percentage loss of material, limiting the number of restarts. An additional unwanted complication was the necessity of a secondary flow path. The micro-hybrid igniter used GOX as oxydizer, while the main motor's oxidizer was nitrous oxide. The presence of multiple oxidizer lines with associated tankage, pressurant, regulators, and valves would be unacceptable on a flight-weight system. Finally, the design required the delicate machining of multiple channels in a brittle heat-tolerant ceramic insulator. The insulator was very prone to fracture, which could potentially lead to a dangerous short circuit through the GOX propellant line.

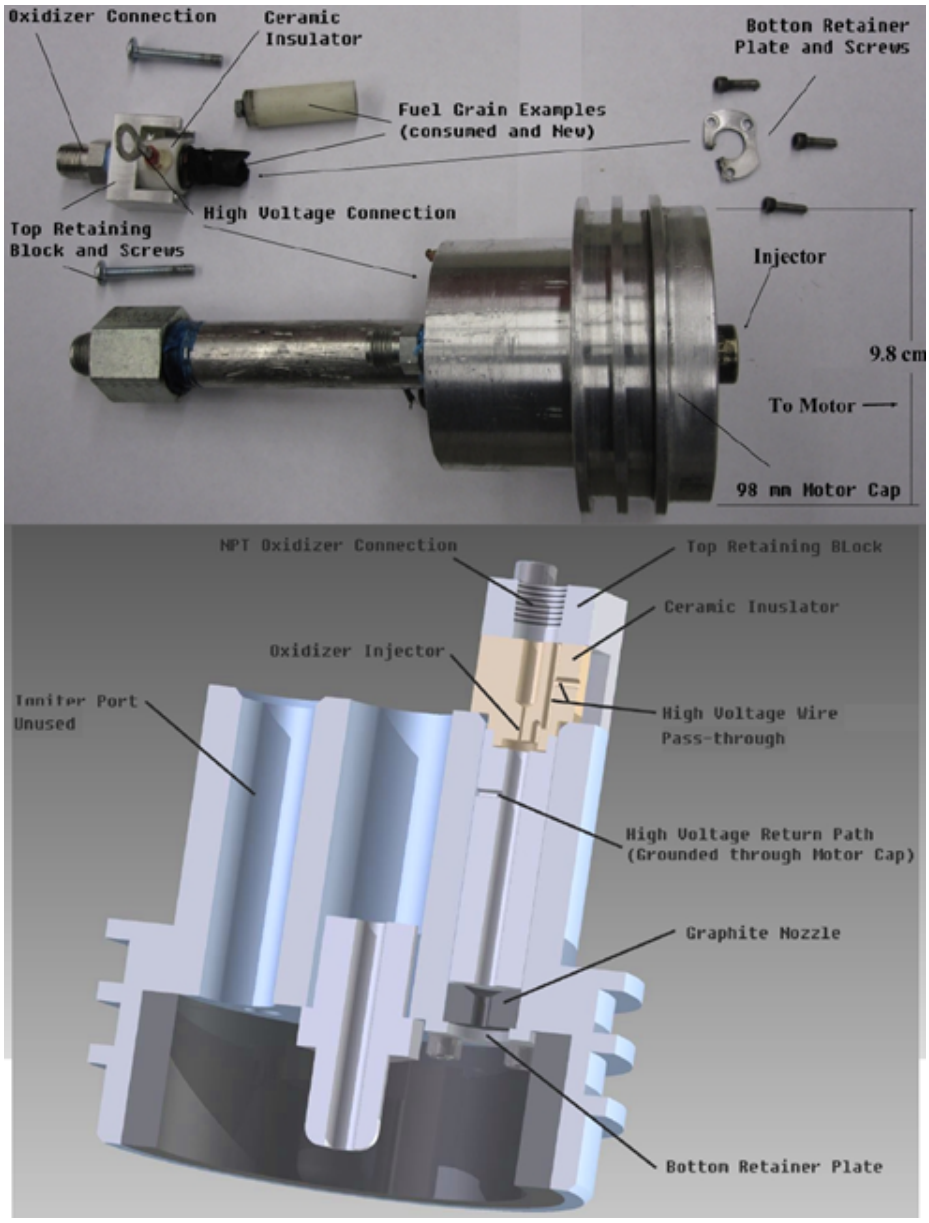

Fig. 5.3: Schematic of micro-hybrid ABS arc igniter motor cap integration.

Fig. 5.4: Test of micro-hybrid ABS arc igniter in 98-mm motor cap.

5.3 Precombustion Chamber-Integrated Igniter

The next group of igniter designs were geared toward addressing the shortcomings of the micro-hybrid. Rather than house a small separate ABS fuel grain in the 98-mm motor cap, channels for conductive paths were built into full-scale additively manufactured precombustion chambers. These precombustion chambers could be "plugged into" a main propellant grain of either HTPB or ABS. With such a system, restarts should be capable within a much greater range of cumulative burn time. Furthermore, a positive connection exists for the return path, there is no secondary oxidizer line, and no components are prone to structural failure. A conceptual drawing of how the precombustion chamber-integrated igniter would be featured in a large hybrid motor is found in Fig. 5.5.

5.3.1 Experimental Apparatus

The previous ABS arc igniter tests were carried out on the USU Propulsion Group's legacy test stand: the Mobile Nitrous oxide Supply and Test Resource cart (MoNSTeR).

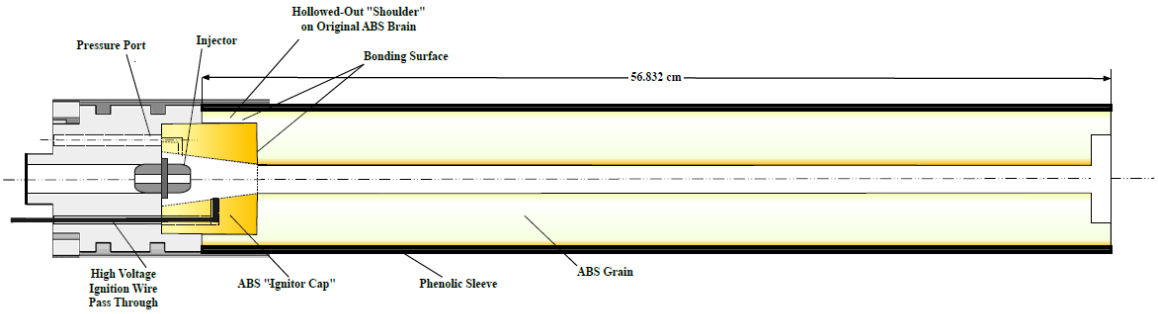

Fig. 5.5: Conceptual diagram for top-level integration of a precombustion chamber-integrated igniter.

Fig. 5.6 gives a view of the MoNSTeR in the jet and rocket propulsion test cell on the USU campus. The MoNSTeR is a modular mobile test stand with integrated propellant tanks, pressurant tanks, and instrumentation. While the MonSTeR is a valuable resource, the integration of the arc igniter subsystems was unsatisfactorily clumsy. For the new round of static firings greater experimental flexibility and a higher testing tempo was desired. Additionally, parallel efforts by the Propulsion Research Group in advancing non-toxic monopropellant technology necessitated the construction of new testing infrastructure. To this end, a new mobile test stand was designed and built: the Kart for Reactive Monopropellant Testing (KRMT). As an ABS arc igniter had been previously envisaged as a prominent element in the non-toxic monopropellant experiments, it was decided that testing of the chamber-integrated igniter on the KRMT would be beneficial for both efforts. An image of the KRMT (as configured for ABS arc igniter testing) is found in Fig. 5.7.

In its igniter testing configuration, the KRMT's instrumentation and controls suite managed via a National Instruments Compact RIO® with an 8-slot NI-compact DAQ® module compatible chassis. Modules used for these experiments included analog in, analog out, TTL command, digital out (relay), and thermocouple. The data acquisition and control tasks were run by a Virtual Instrument programmed in the NI Labview® graphical language in the RT Scan environment. This allowed for a simple and very deterministic data acquisition and controls scheme. Fig. 5.8 shows the view of the testing apparatus from the inside of the test cell's control room.

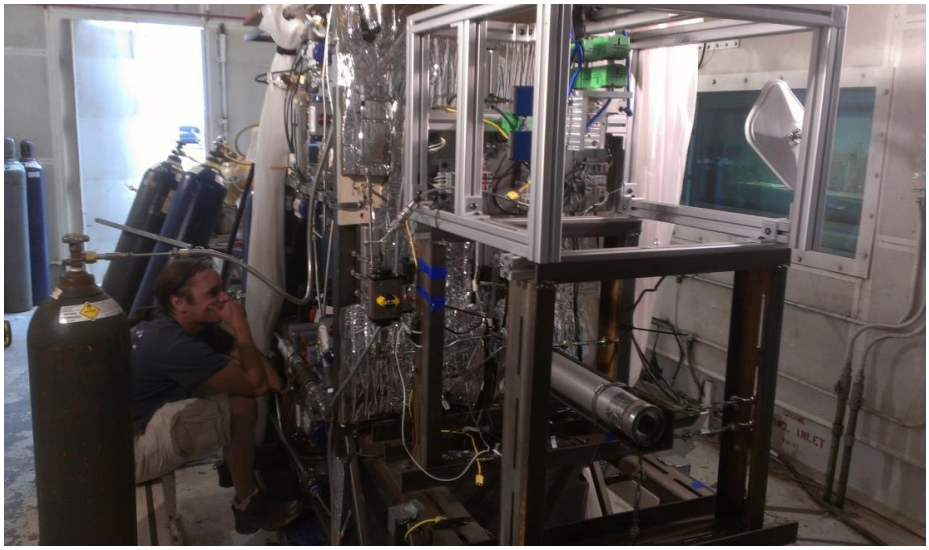

Fig. 5.6: Mobile Nitrous oxide Supply and Test Resource cart.

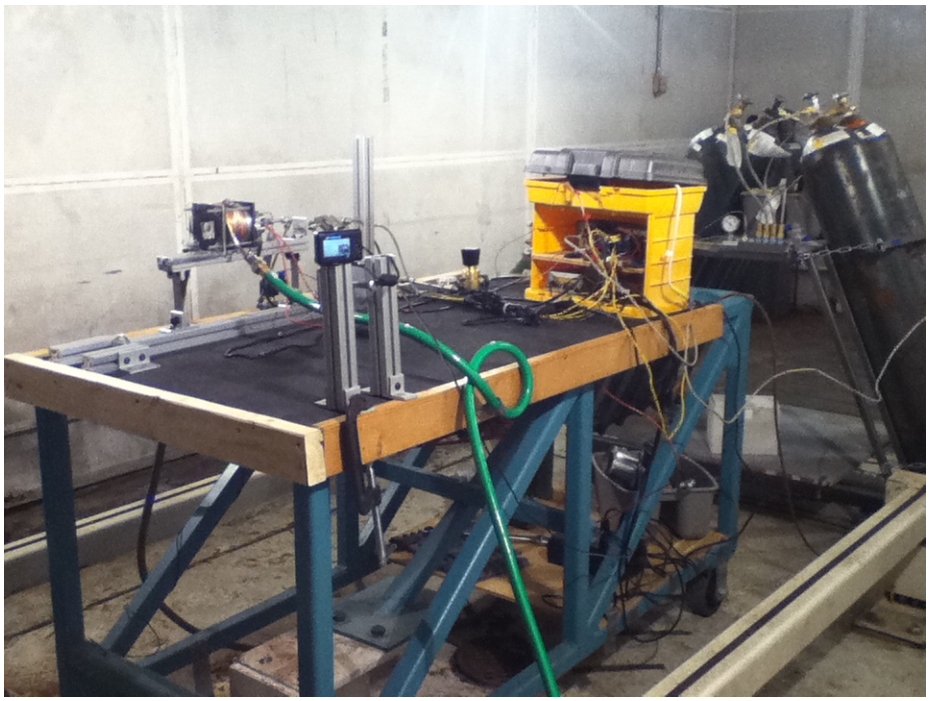

Fig. 5.7: Kart for Reactive Monopropellant Testing.

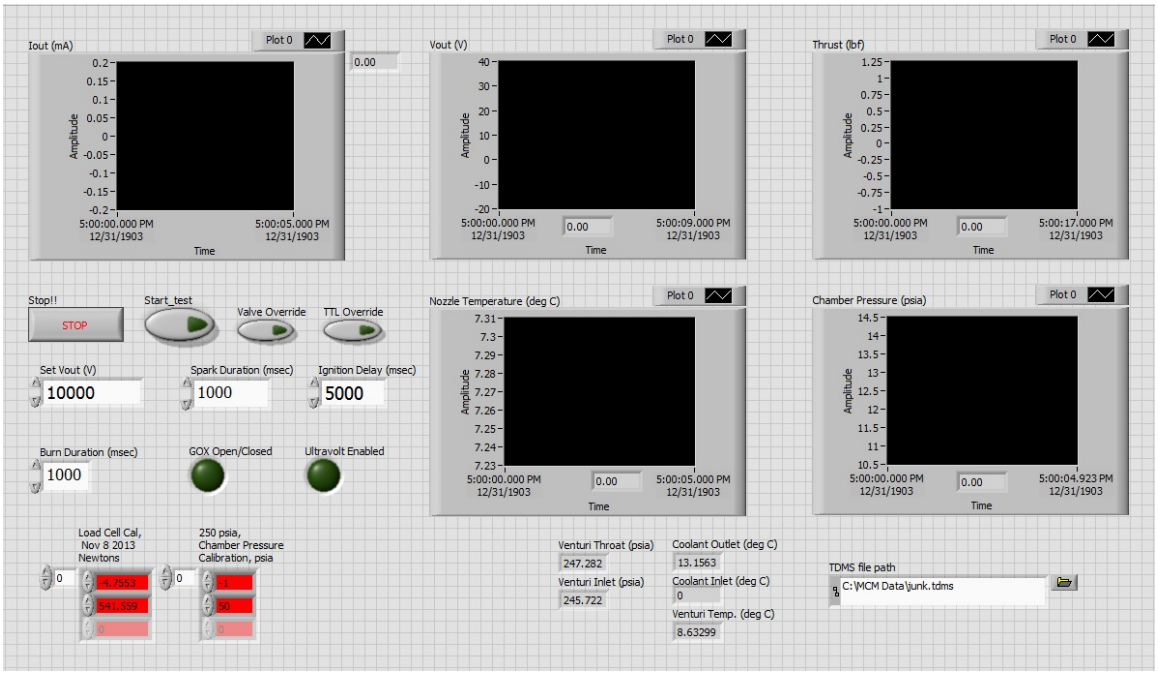

Fig. 5.8: Operator's graphical interface for ABS arc igniter testing.

Acquired input channels included venturi pressures (inlet and throat), chamber pressure, upstream and downstream coolant temperatures, igniter case temperature, venturi temperature (necessary for determining GOX density in the venturi), and thrust. Among the output channels were a TTL enable signal to activate the HVPS, analog out $(0-5\ V)$ to modulate the maximum voltage delivered by the HVPS, and digital out to fire the GOX solenoid valve.

Once again, GOX was chosen as the igniter's oxidizer. The GOX supply was contained in a type-B gas cylinder, downstream of which was a variable-pressure regulator. Downstream of the regulator was a custom designed and built venturi flowmeter for mass flow rate measurement. Flow in the line was controlled in a boolean fashion by a GOX-safe solenoid valve. Fig. 5.9 displays a plumbing and instrumentation diagram for arc igniter testing on the CRMT. A view of the CRMT thrust stand is shown in Fig. 5.10.

5.3.2 Converging Section Igniter

The geometry of the first precombustion chamber-integrated fuel grain represented a

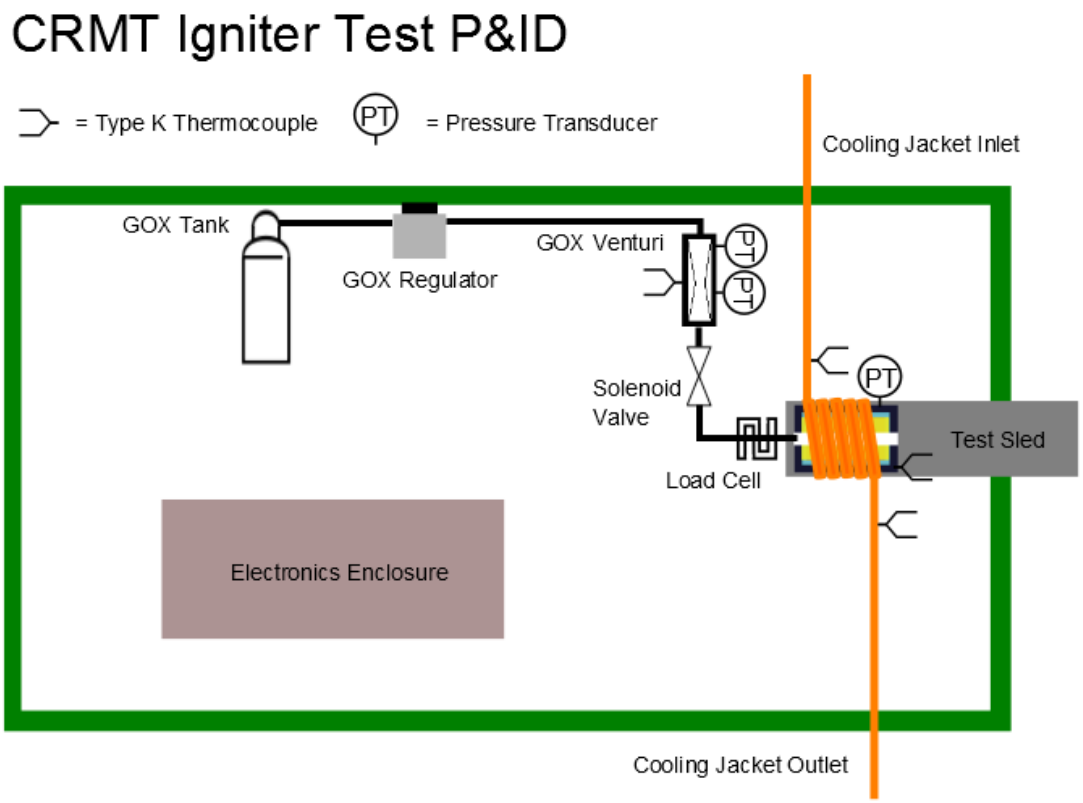

Fig. 5.9: Plumbing and instrumentation diagram for the CRMT in igniter testing configuration.

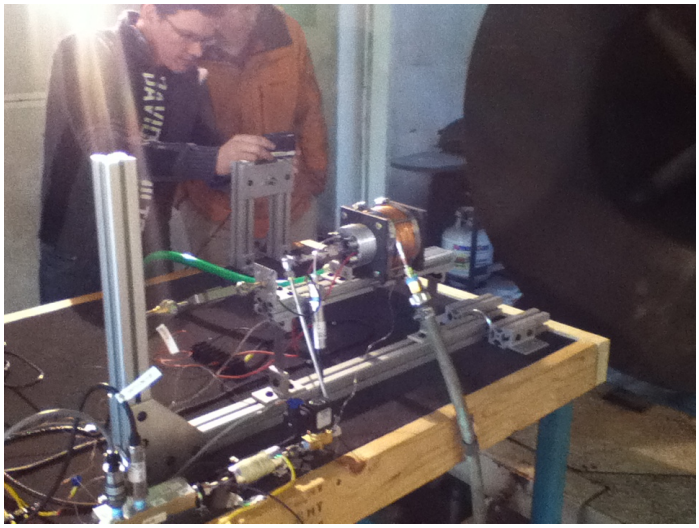

Fig. 5.10: CRMT thrust stand.

worst-case scenario for achieving ignition. The high tension lead and return path were placed exactly opposite one another, reducing electric field strength for a given supply voltage. The port of the grain was shaped to act as a subsonic nozzle. The flow within such a grain would exhibit no recirculation zones and would be moving relatively swiftly, effectively decreasing the fuel vapor concentration in the arc region and slowing reaction kinetics. Fig. 5.11 shows one of these igniter grains after several spark tests, but before full ignition testing took place.

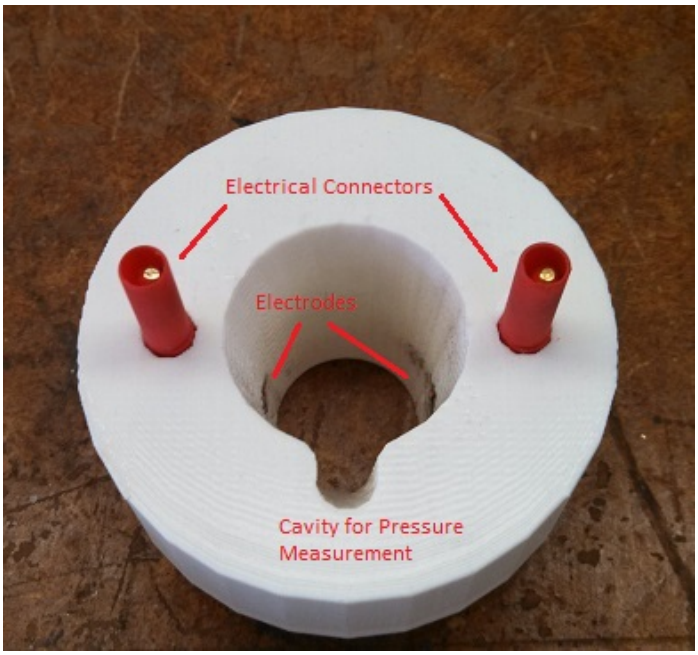

Fig. 5.11: Converging section ABS fuel grain.

Three grains with this geometry were manufactured: two were printed and the other was machined from extruded ABS stock material. Before integration on the thrust stand, the arcing characteristics of the grains was observed. Both of the printed ABS grains produced substantial gas breakdown and hydrocarbon vapor generation, but the breakdown was not achieved with the machined grain.

After having successfully carried out dozens of breakdown cycles, one of the grains ceased to arc. Instrumentation indicated that the HVPS was still limiting current, indicating a short circuit of some sort. Indeed, when the grain was disassembled and cut into halves a

wire forming the conductive path to one of the electrodes was found to be broken. Fig. 5.12 shows a cross-sectional view of the grain. The patterns of heavy char indicate that electrical breakdown was occurring between the wire and the aluminum case, rather than along the inner surface of the oxidizer port.

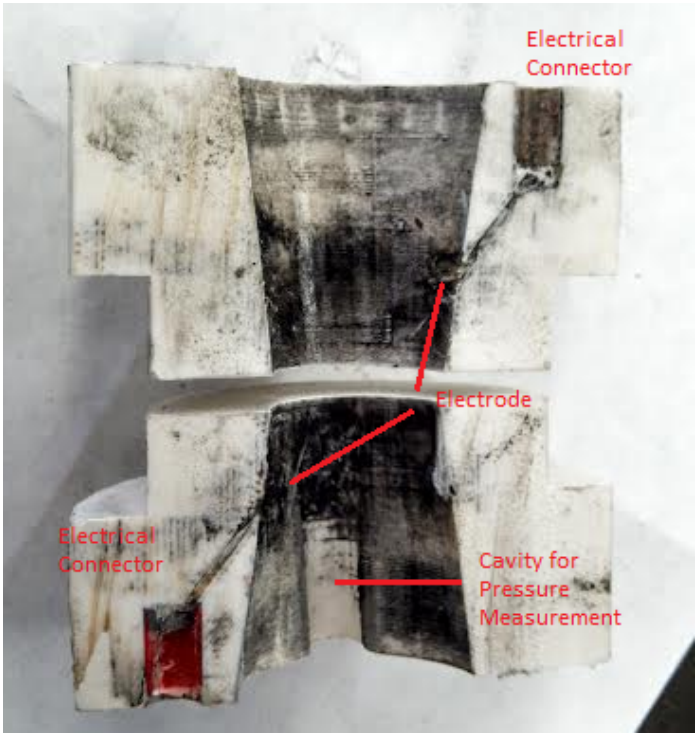

Fig. 5.12: Cross section of compromised ABS igniter grain.

The primary motivation for adopting the precombustion chamber-integrated form factor was for streamlined integration on a large motor, but testing such system in full was deemed too cumbersome for carrying out tests in rapid succession. As an alternative, supplemental measures were taken to effectively convert an existing 98-mm motor cap into a small hybrid motor whose internal conditions matched those of the full-scale motor. This significantly reduced the complexity of test operations and dramatically increased the number of ignition cycles that could be run. The design was engineered such that nozzle geometries could be varied to provide a range of internal chamber conditions. Additionally, GOX injection pressure could also be modulated.

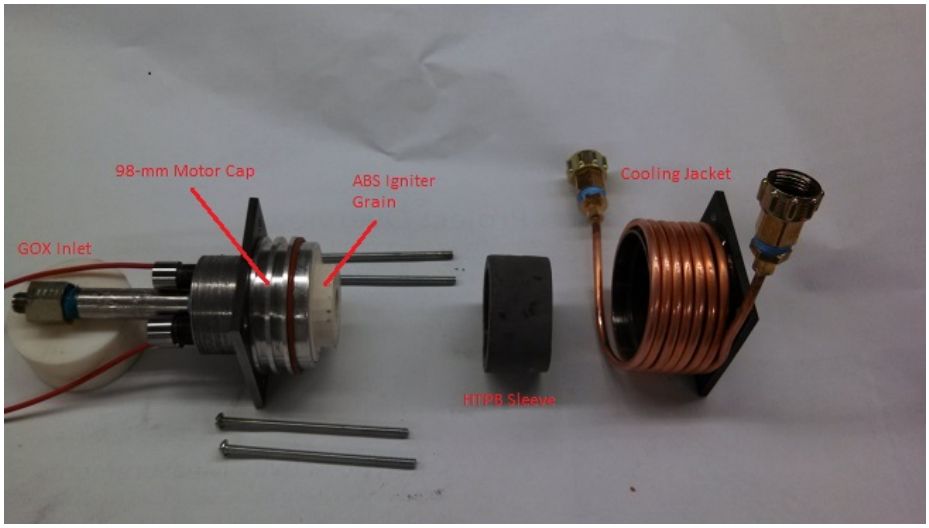

Fig. 5.13: Exploded view of the precombustion chamber-integrated igniter test motor.

When fully integrated inside the small test motor setup, ignition was not achieved under conditions similar to those in a full 98-mm motor.

At this point, an extremely small (1/16 in) nozzle was fitted to the test motor in order to cause choking flow conditions in the combustion chamber. Then, by changing the input pressure of the GOX, initial chamber pressure could be modulated. A series of tests were performed for a range of initial chamber pressures. Successful ignition was observed for all cases in which initial chamber pressure exceeded approximately 20 psi.

5.3.3 Shelf Igniter

Another round of igniter grains were manufactured, taking lessons from the test data for those with the converging oxidizer port. The new design was based on a more traditional precombustion chamber geometry. The conductive math was significantly changed such that the distance between the electrodes was reduced, thereby increasing electric field strength. The electrodes themselves were housed at the root of a "shelf" feature in an effort to cause flow stagnation and increase local pressure in the vicinity of the arc. A larger nozzle was used to prevent chamber pressure from rising up to injector pressure, as had happened in the previous round of tests. Fig. 5.18 shows this geometry. Fig. 5.19 shows the igniter grain after the test series was completed.

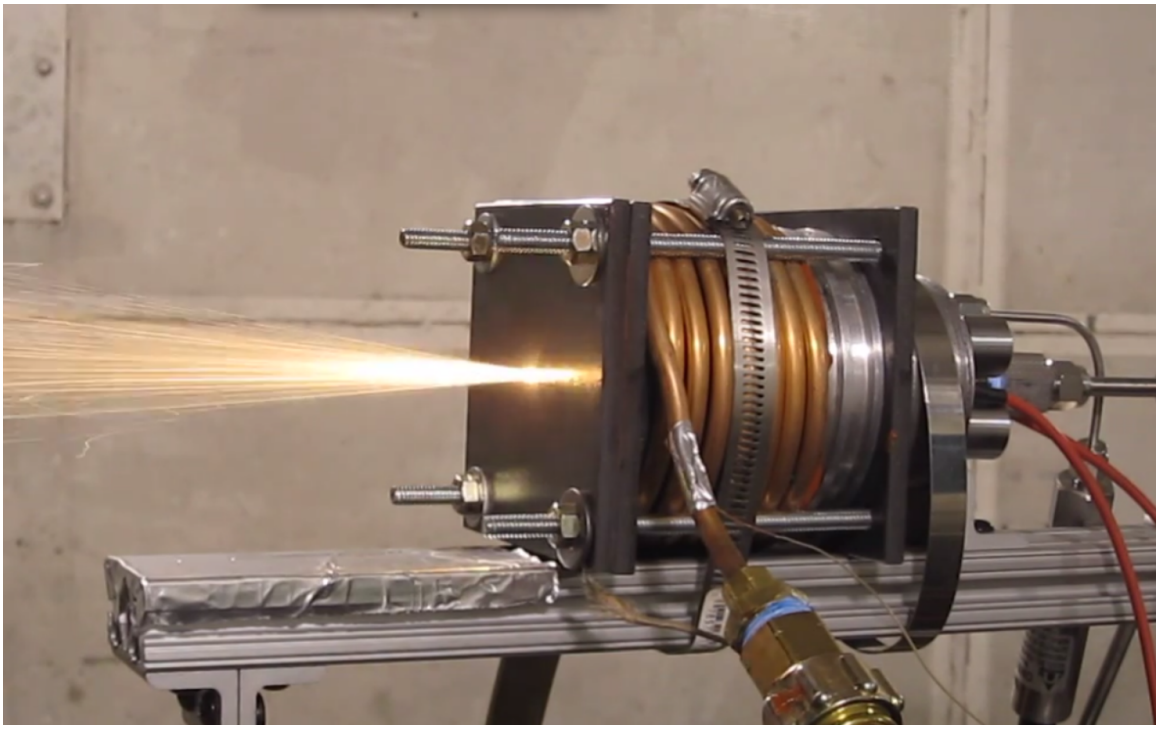

Fig. 5.14: Still image from converging section igniter grain testing.

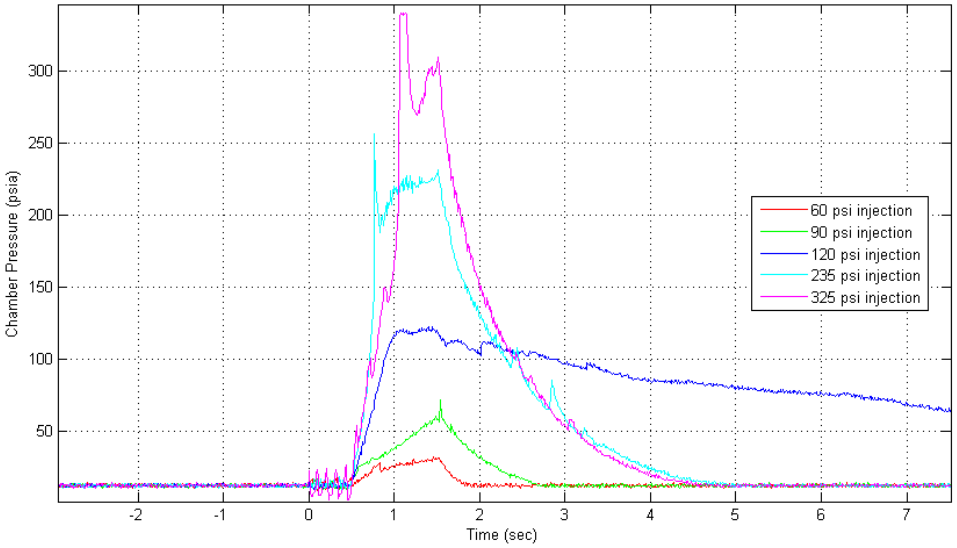

Fig. 5.15: Chamber pressure measurements for converging section igniter grain.

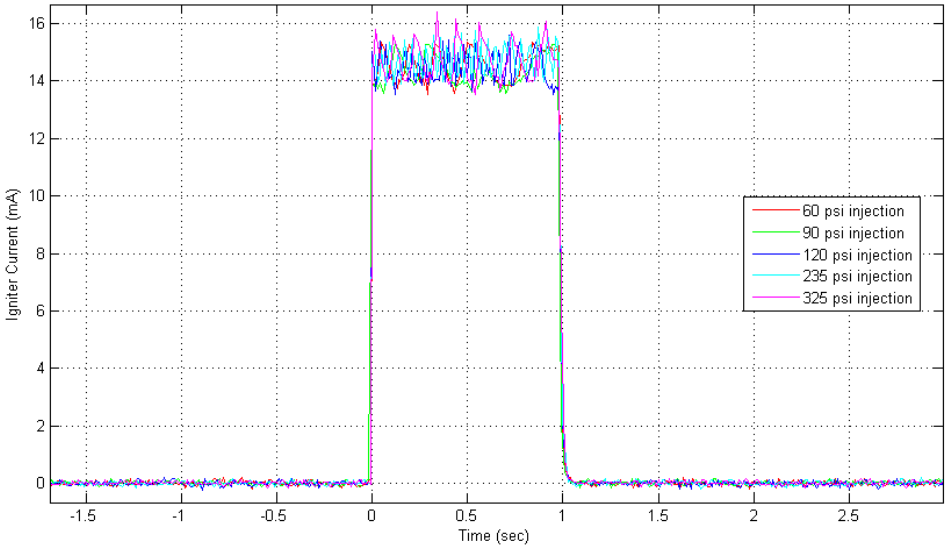

Fig. 5.16: Igniter current measurements for converging section igniter grain.

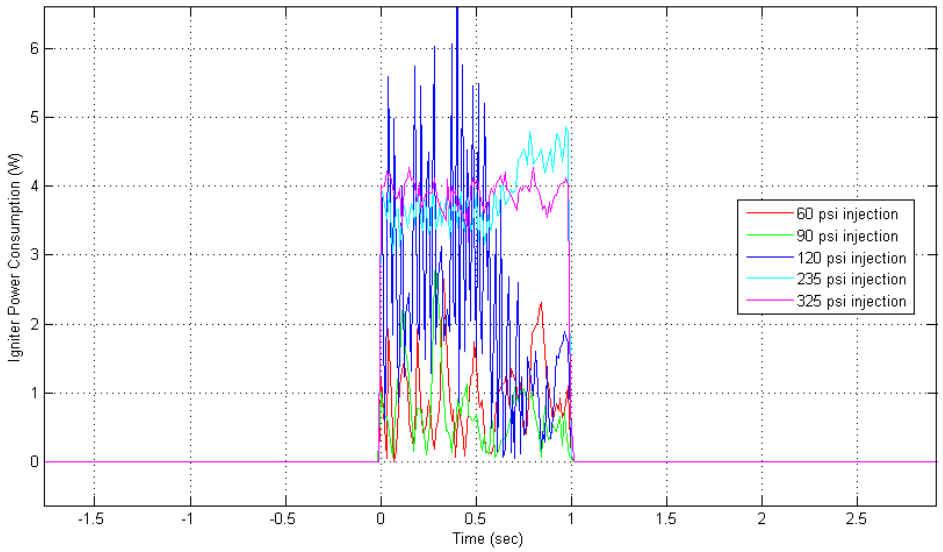

Fig. 5.17: Igniter power consumption measurements for converging section igniter grain.

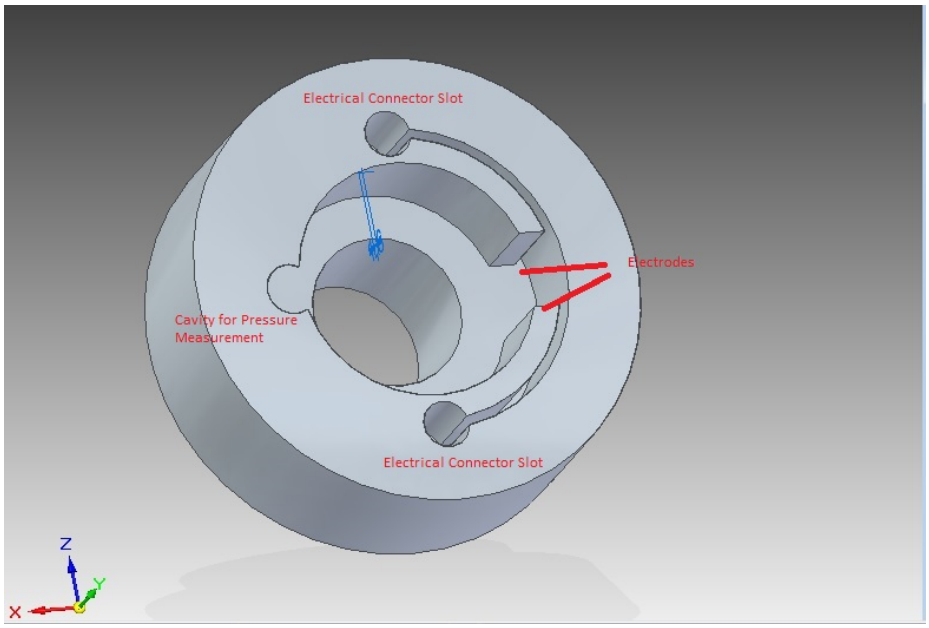

Fig. 5.18: Electrode shelf ABS igniter grain.

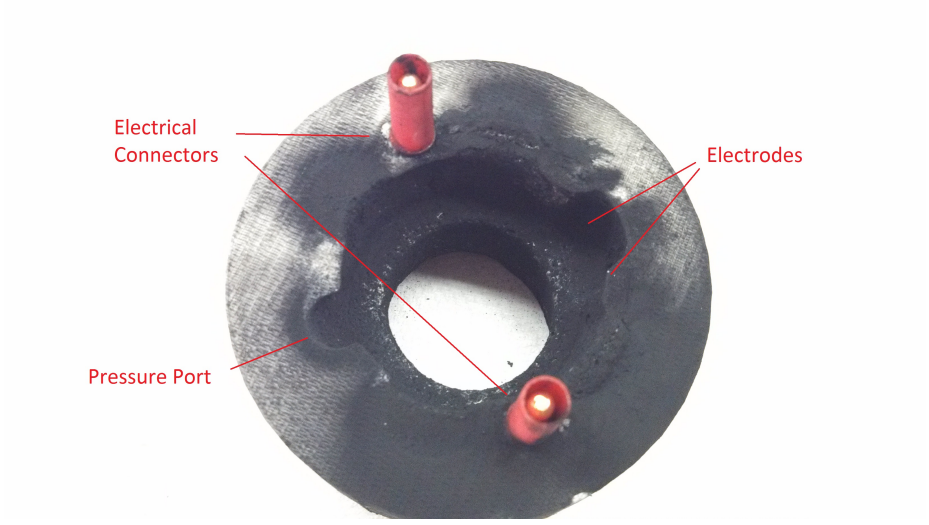

Fig. 5.19: Post-disassembly electrode shelf ABS igniter grain.

As before, a series of ignition tests were performed for a range of initial chamber pressures. The same patterns were observed; ignition did not take place for initial chamber pressures less than 20 *psi*. This implies that no significant pressure increase was present near the electrodes. Computational fluid dynamics analysis carried out after the burns indicates that injector plume impingement on the shelf was unlikely, explaining the experimental results.

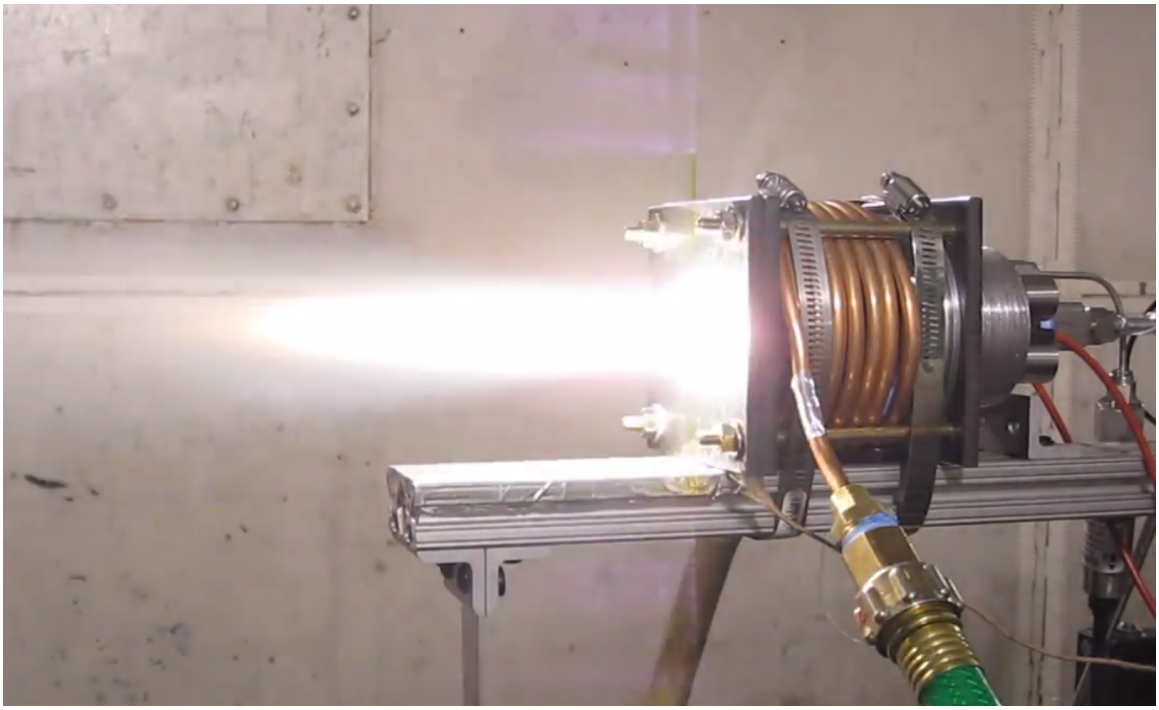

Fig. 5.20: Still image from shelf igniter grain testing.

5.4 Discussion of Results

The data provided by the experiments described in the preceding chapter carry several important implications. Primarily, they demonstrate the fundamental feasibility of the ABS arc igniter concept. Upon reviewing the data, a threshold can be seen for successful ignition requiring pressures between $20 - 30$ *psia* near the breakdown event. This is most likely a limitation of the reaction kinetics of ABS/GOX combustion. This is far from difficult to achieve–even in an un-choked combustion chamber.

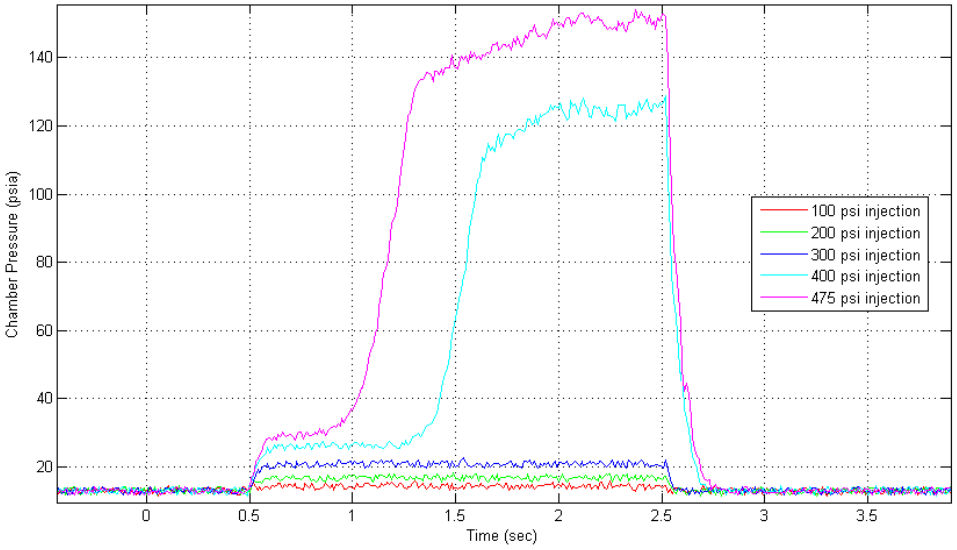

Fig. 5.21: Chamber pressure measurements for shelf igniter grain.

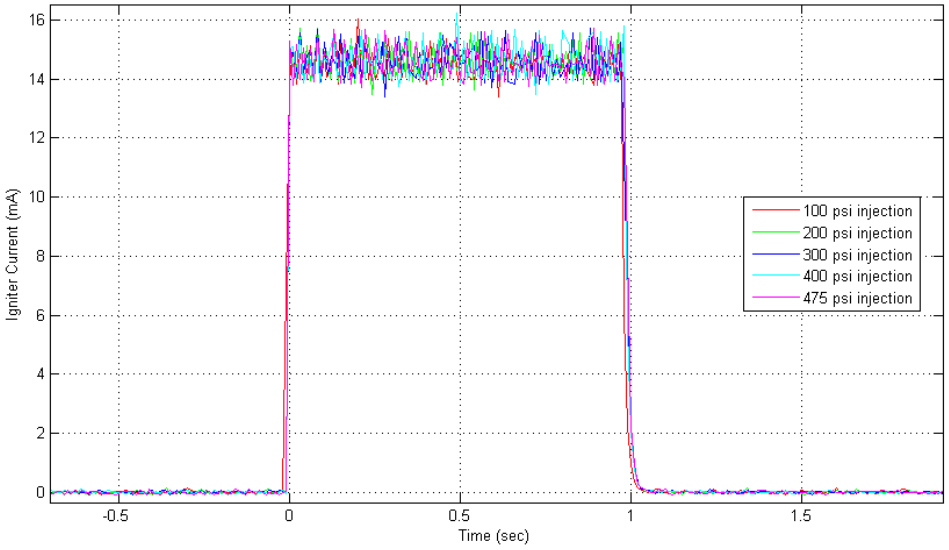

Fig. 5.22: Igniter current measurements for shelf igniter grain.

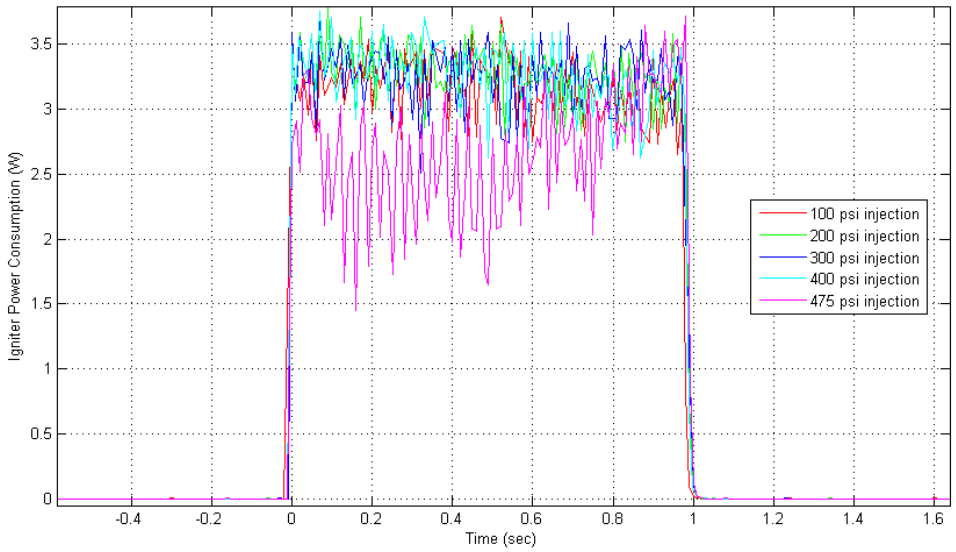

Fig. 5.23: Igniter power consumption measurements for shelf igniter grain.

In preparation for this paper, a rough calculation of power output for the most recent ignition tests was made. The calculation was based on the propellant mass flow rate, constant-pressure specific heat, and combustion flame temperature as seen in the following equation:

$$P_{out} = \dot{m} c_p T_0 \tag{5.1}$$

The combustion properties necessary to carry out the calculation were found with the assistance of NASA's industry standard equilibrium chemistry code "Chemical Equilibrium with Applications." An oxidizer-to-fuel ratio of 12 was chosen based on post-test fuel mass measurements. The mass flow rate calculation was based on the measured chamber pressure and calculated combustion flame temperature.

According to these power output calculations, ABS arc igniter systems are able to provide tens of thousands of Watts of power from an input of a mere $3 - 5\ W$. It should be noted that this is accomplished with components that present absolutely no toxic or detonation hazards. Fig. 5.24 shows the calculated power output for the precombustion chamber-integrated igniter alongside its power consumption.

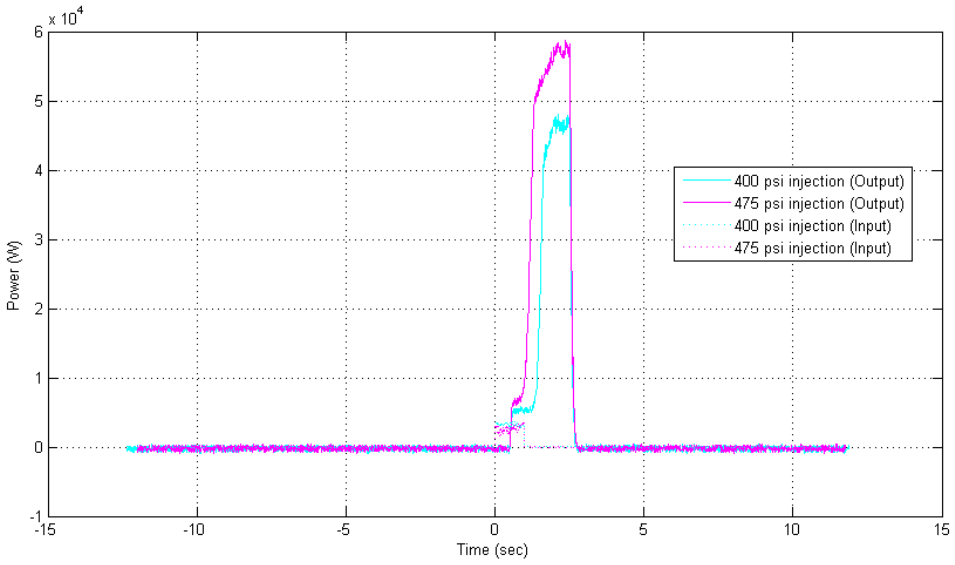

Fig. 5.24: Power output for shelf grain.

Chapter 6

Conclusion

6.1 Summary

In comparison to other methods of propulsion, the state-of-the-art of rocket ignition–especially hybrid rocket ignition–is somewhat crude. Most igniters are not restart-capable, and those that are usually involve the handling of very hazardous materials. As society has become more safety and environment-conscious, significant impetus has accumulated for the development of alternative ignition systems.

Members of the USU Propulsion Research group happened upon the unique electrical breakdown characteristics of ABS plastic while investigating its use as a hybrid rocket fuel. Under a sufficiently high voltage, gas and solid breakdown occur, yielding high temperatures and the generation of fuel vapor. This phenomenon was used as the basis for a series of experimental ABS arc igniters. The igniters were designed, built, and tested successfully. The research program successfully demonstrated the ability to restart hybrid motors multiple times with the press of a button. The prototype undertook nearly thirty restart cycles, the microhybrid igniter performed four while integrated on a large-scale motor, and each of the precombustion chamber-integrated igniter designs carried out 10+ cycles. This was accomplished without any hardware exchange between burns. Requirements for minimum operating conditions were established. An estimate of delivered power was made, indicating a power amplification factor on the order of 10^4!

The serious development of the ABS arc igniter concept may carry staggering implications for the future of hybrid rocketry. As discussed in Chapter 1, the ability to restart hybrid rocket motors is desirable in a wide range of applications, from sub-orbital space tourism to small satellite propulsion to even manned spaceflight. The high enthalpy output of the igniter indicates potential as a gas generator. Finally, the ABS arc igniter involves

cheap, safe, materials and manufacturing processes, providing the means for small research organizations to include significant maneuvering capability on their spacecraft.

6.2 Suggestions for Future Work

ABS arc igniter research has raised many questions about the physical mechanisms behind its enabling features. Chief among them is the determination of the pyrolysis characteristics of ABS plastic. Chemical equilibrium calculations indicate that lower oxidizer to fuel ratios at ignition could ease the minimum ignition pressure requirement. A firm characterization of ABS's pyrolysis and electrical breakdown may unveil igniter design rules that enhance the production of hydrocarbon vapor during arcing and thus enable the creation of oxidizer to fuel ratios that more closely approach stoichiometric.

Currently, the reasons for which ABS plastic can–unlike other hybrid fuels–be used as an electrode for electrical gas breakdown are not well understood. Further research into the materials science that makes such behavior possible may assist in the design of ABS (or other solid hydrocarbon) formulations that are best suited to this application.

Nitrous oxide is the most commonly used oxidizer for hybrid rocket motors. Up to this point, ABS arc ignition using nitrous oxide has not yet been attempted, though it is thought that such a demonstration should not be difficult. As an important step in increasing the credibility of ABS arc ignition, demonstration of an igniter using nitrous oxide oxidizer should be performed.

The efficacy and novelty of the igniter would be most sensationally demonstrated in a flight campaign. The use of in-flight ABS arc ignition on the second-stage of a sounding rocket would advance acceptance of the technology and lead to greater investment.

Finally, because of the massive amount of enthalpy generator for such a small power input, the ABS arc igniter is currently be investigated at USU as a means of inducing thermal decomposition of a non-toxic replacement for hydrazine [24]. The monopropellant of interest is hydroxylammonium nitrate (HAN), and ammonia salt normally stored as an ionic solution in water. Traditional catalytic HAN decomposition approaches require a preheat cycle that consumes 30 W for several minutes prior to any maneuver. This carries

serious consequences for spacecraft with small power budgets [25]. The ABS arc igniter, in contrast, only requires $3 - 5\ W$ over a fraction of a second. Development of the igniter technology in this context may prove to be a boon to the small satellite community.

References

[1] Sutton, G. P., and Biblarz, O., *Rocket Propulsion Elements*, Wiley, 2010.

[2] DeSain, J. D., "Green Propulsion: Trends and Perspectives," *Crosslink, http://www.aero.org/publications/crosslink/summer2011/04.html*, [retrieved 21 March, 2012].

[3] Sittig, M., *Handbook of Toxic and Hazardous Chemicals and Carcinogens*, Noyes Publications, 2nd ed., 1985.

[4] Thicksten, Z., "Handling Considerations of Nitrous Oxide in Hybrid Rocket Motor Testing," *44th AIAA/ASME/SAE/ASEE Joint Propulsion Conference & Exhibit, July 2008, Hartford, CT*.

[5] Peterson, Z., Eilers, S. D., and Whitmore, S., "Closed-Loop Thrust and Pressure Profile Throttling of a Nitrous-Oxide HTPB Hybrid Rocket Motor," *AIAA 2012-4551*, 2012.

[6] Lu, F. K., *Fundamentals of Hybrid Rocket Combustion and Propulsion*, American Institute of Aeronautics and Astronautics, Inc., 2007.

[7] "Dream Chaser Commercial Crewed Spacecraft Overview," *17th AIAA International Space Planes and Hypersonics Systems and Technologies Conference, April 2011, San Fransisco California*.

[8] Borman, G. L., and Ragland, K. W., *Combustion Engineering*, McGraw-Hill, 1998.

[9] Anderson, J. D., *Modern Compressible Flow with Historical Perspective*, McGraw-Hill, 2003.

[10] Seamans, T. F., Vanpee, M., and Agosta, V. D., "Dvelopment of a Fundamental Model of Hypergolic Ignition in Space-Ambient Engines," *AIAA*, Vol. 5, 1967.

[11] Jr., H. J. D., "NASA Fastrac Engine Gas Generator Component Test Program and Results," *36th AIAA/ASME/SAE/ASEE Joint Propulsion Conference*, 2000.

[12] Caveny, L. H., Kuo, K. K., and Shackelford, B., "Thrust and Ignition Transients of the Space Shuttle Solid Rocekt Motor," *AIAA Journal of Spacecraft*, Vol. 17, 1980.

[13] Hulka, J., Forde, J., and Werling, R., "Modification and Verification Testing of a Russian NK-33 Rocket Engine for Reusable and Restartable Applications," *AIAA 98-3361*, 1998.

[14] Clark, S., "Falcon 9 Engine Restart Glitch Blamed on Thermal Conditions," November 2013.

[15] Bonanos, A. M., "Combustion Experiments with an Integrated Aeroramp-Injector/Plasma-Torch Igniter," *Journal of Propulsion and Power*, Vol. 24, 2008, pp. 267–273.

[16] Musk, E., "SpaceX News," May 2005.

[17] Kuffel, E., Zaengl, W., and Kuffel, J., *High Voltage Engineering Fundamentals*, Newnes, 2000.

[18] Townsend, J. S. E., *Electricity in Gases*, Clarendon Press, 1915.

[19] Naidu, M., *High Voltage Engineering*, McGraw-Hill, 1996.

[20] Stratasys®, "Mechanical Properties of ABS Plastic," 2007.

[21] Feldman, J., "Plastics - Materials of the 21st Century," *BASF News Releases*, 2011.

[22] Eilers, S. D., Whitmore, S. A., and Peterson, Z. W., "Development and Testing of the Regeneratively Cooled Multiple Use Plug Hybrid (for) Nanosats (MUPHyN) Motor," *48th AIAA/ASME/SAE/ASEE Joint Propulsion Conference and Exhibit, Altanta, GA*, 2012.

[23] Whitmore, S. A., Peterson, Z. W., and Eilers, S. D., "Analytical and Experimental Comparisons of HTPB and ABS as Hybrid Rocket Fuels," *47th AIAA/ASME/SAE/ASEE Joint Propulsion Conference & Exhibit*, 2011.

[24] Whitmore, S. A., Merkley, D. P., Eilers, S. D., and Judson, M. I., "Development and Testing of a Green Monopropellant Ignition System," *48th AIAA/ASME/SAE/ASEE Joint Propulsion Conference, San Jose, CA*, 2013.

[25] Spores, R. A., Masse, R., and Kimbrel, S., "GPIM AF-M315E Propulsion System," *48th AIAA/ASME/SAE/ASEE Joint Propulsion Conference, San Jose, CA*, 2013.